Enhancing Network Lifetime in Wireless Sensor Networks Using Multiple Base Stations and Cooperative Diversity

by

Amar Prakash Azad

Department of Electrical Communication Engineering

Indian Institute of Science

BANGALORE – 560 012

January 2006

Acknowledgements

Abstract

A key issue in wireless sensor networks is maximizing the network lifetime. Network lifetime becomes particularly important in sensor networks where the sensor nodes, distributed typically in remote/hostile sensing areas, are powered by finite energy batteries which are not easily replaced/recharged. Depletion of these finite energy batteries can result in a change in network topology or in the end of network life itself. Hence, prolonging the lifetime of sensor networks is of interest.

In sensor networks, the data transport model is such that a base station, typically located at the boundary of or beyond the area in which sensors are distributed, collects data from the sensor nodes. That is, the sensor nodes are the data sources and the base station is the data sink. Typically, the sensor nodes, in addition to behaving as source nodes in generating data to be passed on to the base station, act as intermediate relay nodes as well to relay data from other source nodes towards the base station on a multihop basis. In this thesis, we focus on an approach which uses *multiple base stations* to enhance network lifetime. Deployment of multiple base stations as data sinks can reduce the average number of hops between the source nodes and their corresponding data sinks.

In the first part of the thesis, we address the question concerning the limits on the network lifetime when multiple base stations are deployed along the boundary of the sensing area. Specifically, we derive upper bounds on the network lifetime when multiple base stations are employed, taking into account the region of observation, number of nodes, number of base stations, locations of base stations, radio path loss characteristics, efficiency of node electronics, and energy available in each node. We also obtain optimum

locations of the base stations that maximize these network lifetime bounds. For a scenario with single base station and a rectangular region of observation, we obtain closed-form expressions for the network lifetime bound and the optimum base station location. For the case of two base stations, we jointly optimize the base station locations by maximizing the lifetime bound using a genetic algorithm based optimization. Joint optimization for more number of base stations is complex. Hence, for the case of three base stations, we optimize the third base station location using the previously obtained optimum locations of the first two base stations. We also provide simulation results validating the network lifetime bounds and the optimal choice of the locations of the base stations.

In the second part of the thesis, we consider the problem of deploying multiple mobile base stations at locations from a set of *feasible* base station locations (sites) along the boundary of the sensing area. Given that K, $K \geq 1$ base stations can be deployed, the problem to solve is to choose the optimum locations for these K base stations from the set of feasible sites. We propose energy efficient, low-complexity algorithms to determine optimum locations of the base stations; they include i) Top-K_{max} algorithm, ii) maximizing the minimum residual energy (Max-Min-RE) algorithm, and iii) minimizing the residual energy difference (MinDiff-RE) algorithm. We show that the proposed base stations placement algorithms provide increased network lifetimes and amount of data delivered during the network lifetime compared to single base station scenario as well as multiple static base stations scenario, and close to those obtained by solving an integer linear program to determine the locations of the mobile base stations. We also investigate the additional lifetime gain that can be achieved when an energy aware routing protocol is employed in the multiple base stations scenario.

In the last part of the thesis, we briefly investigate the benefit of employing cooperative diversity in enhancing the lifetime of wireless sensor networks. By considering a single base station scenario and using an amplify-and-forward relay protocol, we illustrate through bounds and simulations the benefit of employing cooperation compared to no cooperation.

Contents

List of Tables

List of Figures

Chapter 1

Introduction

Recent advances in the area of wireless communications and embedded systems have enabled the development of small-sized, low-cost, low-power, multi-functional sensor nodes that can communicate over short distances wirelessly [1],[2]. These sensor nodes represent a significant improvement over traditional sensors, since these sensor nodes perform processing and communication functions in addition to the traditional sensing function. The processing and communication functions embedded in the sensor nodes essentially allow networking of these nodes, which in turn can facilitate sensing function to be carried out in remote/hostile areas. A network of sensor nodes (often referred to as a wireless sensor network) can be formed by densely deploying a large number of sensor nodes in a given sensing area, from where the sensed data from the various sensor nodes need to be transported to a monitoring station often located far away from the sensing area. The transport of data from a source node to the monitoring station can be carried out on a multihop basis, where other intermediate sensor nodes act as relay nodes. Thus, each sensor node, in addition to behaving as a source node, often needs to act as relay a node for data from other nodes in the network. Application scenarios where such wireless sensor networks can be of critical use include battlefield surveillance, habitat/wildlife monitoring/tracking [3],[4],[5], traffic monitoring, pollution/environment monitoring, and nuclear/chemical/biological attack detection [6].

1.1   Finite Battery Source in Sensor Nodes

The wireless sensor nodes are powered by finite-energy batteries (e.g., 1.2 V, < 0.5 AH batteries). Being deployed in remote/hostile sensing areas, these batteries are not easily replaced or recharged. Thus, end of battery life in a node essentially means end of the node life, which in turn can result in a change network topology or in the end of network life itself. Thus, the network lifetime shows strong dependence on battery lifetime. Efficient use of battery energy is hence crucial to enhance the network lifetime. Energy efficient techniques for increasing network lifetime has been an active area of research [8]-[31].

1.2   Energy Efficient Techniques

Energy efficient techniques in wireless sensor networks can be sought on various layers of the protocol stack [8]-[31]. For example, improving energy efficiency using system partitioning (e.g., clustering of sensor nodes) [8],[9], low duty cycle reception (e.g., sleep mode), dynamic voltage scaling (device level savings) [7], energy efficient MAC protocols (link layer) [10], energy aware routing (network layer) [11] have been investigated and widely reported in the literature.

1.2.1   Energy Efficient Routing

A routing protocol that minimizes the total consumed energy to reach the destination is proposed in [11]. The drawback with this approach is that if all the traffic is routed through the minimum energy path to the destination, the batteries in the nodes in that path can be drained out fast. A better objective hence would be to maximize the network lifetime (e.g., maximize the time to partition the network). In [13], the problem of maximizing the time to network partition has been reported to be NP-complete. In [14], the maximum lifetime problem has been identified as a linear programming problem, and therefore solvable in polynomial time. The same problem for the case of nodes having

multiple destinations has been addressed in [15].

Hierarchical Protocols [8],[9],[16]-[20]: Network clustering has been pursued in some routing approaches. Nodes are formed into groups where nodes in a group send their data to their cluster (group) head, and cluster heads in turn communicate to send the data to the sink. This approach is also referred to as hierarchical routing. The cluster heads themselves are sensor nodes. The choice of sensor nodes to play cluster head role can be made based on certain probabilistic rules, proximity to other nodes, and residual energies in the nodes so as to keep the network life long.

LEACH (**L**ow-**E**nergy **A**daptive **C**lustering **H**ierarchy) [8],[9] is one of the first and popular hierarchical routing algorithms for sensor networks. The idea is to form clusters of sensor nodes based on received signal strength and use cluster heads as routers to the sink. This will save energy since individual nodes spend much less energy than cluster heads, and cluster head role is assigned to different nodes based on a probabilistic rule which evenly assigns this role to different nodes. LEACH has been shown to achieve over a factor of seven reduction in energy dissipation compared to direct communication and a factor of 4 to 8 reduction compared to minimum energy routing.

PEGASIS (**P**ower **E**fficient **GA**thering in **S**ensor **I**nformation **S**ystems) [16] is an improvement to the LEACH protocol. Rather than forming multiple clusters, PEGASIS forms chains so that each node in a chain transmits to and receives from a neighbour and only one node in that chain is selected as a leader to transmit to the sink. The chain construction is done in a greedy way. PEGASIS has been shown to outperform LEACH by a factor up to three for different network sizes and topologies. Such gains are achieved through the elimination of overhead caused by dynamic cluster formation in LEACH and by increased data aggregation. PEGASIS however results in more delay for far-off nodes in the chain from the chain leader. This delay issue in LEACH has been addressed in Hierarchical LEACH in [17]. Although the PEGASIS approach avoids the clustering overhead of LEACH, every node needs to be aware of the status of its neighbour so that it knows where to route the data, and this involves overhead for the resulting dynamic topology adjustments.

TEEN (**T**hreshold sensitive **E**nergy **E**fficient sensor **N**etwork) protocol [18] is a cluster-based hierarchical protocol designed to be responsive to sudden changes in the sensed attributes. Such responsiveness is important in time-critical applications. Once the cluster heads are formed, the cluster head broadcasts two thresholds to the nodes. These are hard and soft thresholds for sensed attributes. A node transmits only when its sensed attribute is above the hard threshold by an amount more than the soft threshold, which can reduce the number of transmissions made by the node. Thus, the number of transmissions from a node can be controlled by a proper choice of these thresholds. However, this approach may not be good for applications where periodic reports are needed. APTEEN (**A**da**P**tive TEEN) [19] is an extension to TEEN and aims at both capturing periodic data collections and reacting to time-critical events. TEEN and APTEEN have been shown to outperform LEACH.

Routing based on location information of the nodes (often referred to as location-based routing) have been considered for wireless sensor networks. For example, [21] presents a Geographic Adaptive Fidelity (GAF) protocol, which is an energy-aware location-based routing algorithm designed primarily for mobile ad-hoc networks, but are applicable to wireless sensor networks as well. The Geographic and Energy Aware Routing (GEAR) protocol in [22] is another protocol which uses location information in addition to energy information. Several other energy efficient routing protocols that take into account the residual energy in the nodes have been reported in the literature [23]-[26].

Our focus in this thesis is not on developing energy efficient routing protocols, but to investigate multiple base stations approach and cooperative diversity approach to network lifetime enhancement (which will be elaborated in later subsections in this chapter). We need, however, to employ routing protocols in our system model. For this purpose, we will consider two routing protocols; i) minimum cost forwarding (MCF) routing protocol in [25], and ii) energy aware routing protocol in [15].

1.2.2 Energy Efficient MAC Protocols

In addition to energy savings at the network layer by the use of energy efficient routing algorithms, sensor network lifetime can be enhanced through energy savings at the link layer as well. Toward that end, several media access control (MAC) protocols have been proposed in the literature. Several papers in the literature have considered the suitability of known MAC protocols and their variants for use in sensor nodes. In [20], a TDMA based MAC is used. A collision-free MAC protocol known as SMACS (**S**elf-Organizing **M**edium **A**ccess **C**ontrol for **S**ensor Networks) has been proposed in [27]. A survey of MAC for wireless sensor networks based on collision-based and collision-free protocols is presented in [28]. Collision based MAC protocols (e.g., slotted ALOHA, and carrier sensing MAC protocols) result in wastage of node energy due to collisions. Also, it would be preferred to avoid continuous listening on the receive side since energy spent in the receive electronics can be saved through interrupted listening (e.g., periodic waking up and listening) [29]. Integrated routing and MAC protocols have also been proposed [30],[31].

Again, our focus in this thesis is not the design of energy efficient MAC protocols. In our investigation of multiple base stations approach to enhance network lifetime, we will use the collision-free SMACS protocol in [27] for our system model.

1.3 Multiple Mobile Data Collection Platforms

Apart from the conventional and widely studied energy efficient techniques (energy aware routing, MAC, etc.) discussed in the above, an interesting approach that has been drawing much research attention recently is the use of *multiple mobile data collection platforms (also referred to as data sinks or base stations)* to enhance the lifetime of sensor networks [39]-[48]. This approach is particularly suitable in scenarios where the data transport model is such that the data from sensor nodes need to be passed on to data collecting platforms (i.e., data sinks/base stations). These platforms can be deployed within the sensing area if the sensing area is easily accessible (e.g., pollution

Figure 1.1: Multihop data transport to base stations. a) Single base station scenario, b) Multiple base stations scenario

or traffic monitoring). On the other hand, in case of remote/hostile sensing areas (e.g., battlefield surveillance), these platforms are expected to be deployed only along the boundary of the sensing area or far away from it. The motivation to use multiple data sinks (base stations) and to allow them to move as well is explained in the following two subsections.

1.3.1   Why Multiple Base Stations?

The usefulness of employing multiple base stations (BS) can be illustrated using Figs. 1.1 (a) and (b). Figure 1.1 (a) shows a sensor network with a single BS B_1 deployed along the boundary of the sensing region $\mathcal{R}$, whereas in Fig. 1.1 (b) three BSs B_1, B_2, B_3 are deployed along the boundary and all these three BSs are allowed to act as data sinks. That is, each sensor node can send its data to any one of these three BSs (may be to the BS towards which the cost is minimum). Base stations can communicate among themselves to collate the data collected (energy is not a major concern in the communication between the BSs).

Suppose the routing is done as shown in Figs. 1.1 (a) and (b). It can be seen that in the single BS scenario in Fig. 1.1 (a), the sensor node 6 takes 4 hops to reach BS B_1.

However, in the three BSs scenario in Fig. 1.1 (b), node 6 can reach BS B_3 in just two hops. That is, by having more than one BS as data sinks, the average number of hops between data source-sink pairs. This will reduce the energy spent by a given sensor node for the purpose of relaying data from other nodes towards the BS. This can potentially result in increased network lifetime as well as larger amount of data delivered during the network lifetime.

In [32], Gandham *et al* investigated the multiple BS approach where they formulated the problem of choosing locations for the BSs as an optimization problem which they solved using a integer linear program (ILP). They showed that the network lifetime can be enhanced using multiple BSs. However, the fundamental question of the limits on the network lifetime achieved for multiple BSs scenario has not been addressed before. For the case of single BS scenario, this question has been addressed by Bhardwaj *et al* in [33],[34], where they have derived analytical upper bounds on the network lifetime. Other papers which are concerned with lifetime bounds for single BS scenario include [35]-[38].

In this regard, our new contribution in this thesis (in Chapter 2) is that we derive upper bounds on the lifetime of sensor networks with multiple base stations [48], taking into account the region of observation, number of nodes, number of base stations, locations of base stations, radio path loss characteristics, efficiency of node electronics, and energy available in each node. In addition, we obtain optimum locations of the base stations that maximize these lifetime bounds.

1.3.2   Why Move Base Stations?

Another interesting idea is to allow the BSs to move for the purpose of reducing the energy spent by the sensor nodes to transport their data to the BS [39]-[45]. If the BSs are allowed to move, possibly close to the sensor nodes, and if the data collection from a given node (or a group of nodes) takes place only when the BS goes near to that node (or that group of nodes) then the transmit energy required at the sensor nodes can get significantly reduced which can substantially increase the network lifetime. The tradeoff

here is that the delay incurred in the data transport may be increased because the nodes have to wait till the BS comes near to them. This moving BS idea has been a topic of recent investigations; Shah *et al* refer the moving data sinks as *'Data Mules'* [40], Somasundara *et al* refer to them as *'Moving Elements'*, and Zhao *et al* refer this idea as *'Message Ferrying* [41],[42]. All these recent works have highlighted the performance benefits of employing moving BSs.

In this thesis (Chapter 3), we investigate the moving BSs approach by considering the following system model. Instead of allowing the BSs to go near the sensor nodes (due to, for example, the sensing area being hostile/inaccessible), the BSs are allowed to dynamically change their locations chosen from a set of *feasible BS locations* (refer to them as 'feasible sites') along the boundary of the sensing area. Suppose there are K, $K > 1$ BSs, and N, $N > K$ feasible sites. The problem to solve is to dynamically choose the optimum locations for the K BSs from the N feasible sites that maximize the network lifetime. We propose three low complexity algorithms for such BS placement. We consider the residual energy in the sensor nodes in choosing the optimum BS locations. We show that the proposed algorithms result in enhanced network lifetime.

1.4 Cooperative Diversity

Recently, cooperative communication techniques have received increased research attention, owing to the potential performance benefits they can offer [54],[55],[56]. In this thesis, we investigate the benefits of cooperative communication techniques in enhancing the lifetime of wireless sensor networks. To motivate this possibility, consider a simple three node network as shown in Fig. 1.2.

A source node S wants to communicate with a destination node D. In a non-cooperative communication context, S would directly transmit to D. In a cooperative communication context, however, the relay node R can receive the transmission from S and forward it to D. This cooperative relaying essentially can provide a diversity path for D to demodulate data from S by observing the transmissions of both S as well as R.
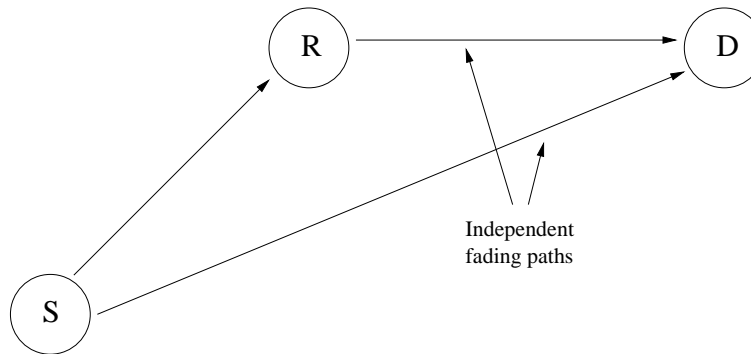
Figure 1.2: Cooperative diversity scheme

Diversity gains can be achieved depending on the location of the relay node as well as the channel characteristics between S to R, S to D, and R to D. It is possible that the participation of the relay node can hurt the performance, particularly if the S to R link is of poor quality. Hence, use of relay node(s) for cooperation must be done judiciously. If multiple relays are used, it can essentially create multiple diversity paths for D. The diversity gains due to combining multiple diversity paths can reduce the transmit energy required (compared to no cooperative diversity) for a desired bit error performance on the link. This reduced transmit energy at the nodes can result in increased network lifetime. In this thesis (in Chapter 4), we investigate the network lifetime enhancement benefit of cooperative diversity.

1.5 Contributions in this Thesis

Motivated by the possible network lifetime enhancement benefits through the use of multiple mobile base stations and cooperative diversity in wireless sensor networks described in the above, we focus on three topics in this thesis, namely,

- Derivation of upper bounds on the network lifetime for the multiple base stations scenario (Chapter 2).

- Development of algorithms for placement of base stations in a mobile base stations

scenario and performance evaluation (Chapter 3).

- Investigation of cooperative diversity for network lifetime enhancement (Chapter 4).

The interesting results and new contributions in these topics can be summarized as follows.

1. In Chapter 2, we address the question concerning the limits on the network lifetime when multiple base stations are deployed along the boundary of the sensing area. Specifically, we derive upper bounds on the network lifetime when multiple base stations are employed, taking into account the region of observation, number of nodes, number of base stations, locations of base stations, radio path loss characteristics, efficiency of node electronics, and energy available in each node. We also obtain optimum locations of the base stations that maximize these network lifetime bounds. For a scenario with single base station and a rectangular region of observation, we obtain closed-form expressions for the network lifetime bound and the optimum base station location. For the case of two base stations, we jointly optimize the base station locations by maximizing the lifetime bound using a genetic algorithm based optimization. Joint optimization for more number of base stations is complex. Hence, for the case of three base stations, we optimize the third base station location using the previously obtained optimum locations of the first two base stations. We also provide simulation results validating the network lifetime bounds and the optimal choice of the locations of the base stations.

2. In Chapter 3, we consider the problem of deploying multiple mobile base stations at locations from a set of *feasible* base station locations (sites) along the boundary of the sensing area. Given that K, $K \geq 1$ base stations can be deployed, the problem to solve is to choose the optimum locations for these K base stations from the set of feasible sites. We propose energy efficient, low-complexity algorithms to determine optimum locations of the base stations; they include i) Top-K_{max} algorithm, ii)

maximizing the minimum residual energy (Max-Min-RE) algorithm, and *iii*) minimizing the residual energy difference (MinDiff-RE) algorithm. We show that the proposed base stations placement algorithms provide increased network lifetimes and amount of data delivered during the network lifetime compared to single base station scenario as well as multiple static base stations scenario, and close to those obtained by solving an integer linear program to determine the locations of the mobile base stations. We also investigate the additional lifetime gain that can be achieved when an energy aware routing protocol is employed in the multiple base stations scenario.

3. In Chapter 4, we investigate the benefit of employing cooperative diversity in enhancing the lifetime of wireless sensor networks. By considering a single base station scenario and using an amplify-and-forward relay protocol, we illustrate through bounds and simulations the benefit of employing cooperation compared to no cooperation.

1.6 Organization of the Thesis

The rest of this thesis is organized as follows. In Chapter 2, we derive upper bounds on network lifetime when multiple base stations are employed in wireless sensor networks. In Chapter 3, we present the study on base stations placement algorithms in a multiple mobile base stations scenario. In Chapter 4, we present the study on cooperative diversity in wireless sensor networks. Conclusions are future work are presented in Chapter 5.

Chapter 2

Upper Bounds on Network Lifetime with Multiple Base Stations

In sensor networks, the data transport model is such that a base station, typically located at the boundary of or beyond the field in which sensors are distributed, collects data from the sensor nodes. Typically, the sensor nodes, in addition to behaving as source nodes in generating data to be passed on to the base station, act as intermediate relay nodes as well to relay data from other source nodes towards the base station on a multihop basis. Therefore, while energy will be spent by a node in receiving and forwarding all transit packets, energy thus spent may not add to end-to-end packet delivery (i.e., packets may still have more hops to reach the base station). This can result in reduced network lifetime and efficiency in terms of total amount of data delivered to the base station per joule of energy in the network, particularly when the hop length between the source node(s) and base station gets larger. This problem can be alleviated by the use of *multiple base stations* deployed along the periphery of the field, and allowing each base station to act as a data sink [32]. That is, each sensor node can send its data to any one of these base stations (may be to the base station towards which cost is minimum). Base stations can communicate among themselves to collate the data collected (energy is not a major concern in the communication between base stations). Deploying such

multiple base stations essentially can reduce the average hop length between the source-sink pairs, thus enabling to achieve increased network lifetime and larger amount of data delivered during the network lifetime. A key question of interest in this regard concerns the fundamental limits on the network lifetime when multiple base stations are deployed.

In [32], Gandham *et al* proposed an ILP-based method for routing in sensor networks with multiple base stations, and showed that network lifetime could be significantly increased using multiple base stations. However, they do not focus on theoretical limits on the network lifetime. Several recent works have focussed on deriving bounds on network lifetime [33]-[38]. In [33],[34], Bhardwaj *et al* derived analytical upper bounds on the network lifetime for a single data sink (base station) scenario. Zhang and Hou, in [35], derived lifetime bounds which are independent of power-saving schemes for large networks. In [38], an upper bound on the average network lifetime for a wireless CDMA sensor network where the the base station antenna gain is shaped in such a way that maximizes network lifetime. However, all the above works do not consider lifetime bounds for multiple base stations scenario. Our new contribution in this chapter compared to the above works is that we derive upper bounds on the lifetime of *sensor networks with multiple base stations*, taking into account the region of observation, number of nodes, number of base stations, locations of base stations, radio path loss characteristics, efficiency of node electronics, and energy available in each node. In addition, we obtain optimum locations of the base stations that maximize these lifetime bounds.

For a scenario with single base station and a rectangular region of observation, we obtain closed-form expressions for the network lifetime bound and the optimum base station location. For the case of two base stations, we jointly optimize the base station locations by maximizing the lifetime bound using a genetic algorithm based optimization. Joint optimization for more number of base stations is complex. Hence, for the case of three base stations, we optimize the third base station location using the previously obtained optimum locations of the first two base stations. We also provide simulation results validating the network lifetime bounds and the optimal choice of the locations of the base stations.

The rest of the paper is organized as follows. In Section 2.1, we present the system model. In Section 2.2, we derive upper bounds and optimum locations of base stations. Simulation results and discussions are presented in Section 2.3. Conclusions are given in Section 2.4.

2.1 System Model

We consider the following system model in our study.

2.1.1 Network

We consider a sensor network comprising of sensor nodes distributed in a region of observation $\mathcal{R}$. The nodes are capable of sensing and sending/relaying data to a base station or a set of base stations using multihop communication. We assume that K base stations are deployed along the periphery of the region of observation to collect data from the nodes. Each node performs sensing operation using an integrated sensing device attached to it, generates information out of it, and processes this information to produce data. It is this data which needs to be sent to the base station(s). At any given instant, the nodes are characterized as dead or alive depending on the energy left in their batteries as being below or above a usable threshold. Live nodes participate in sensing as well as sending/relaying data to the base station(s). While relaying data as an intermediate node in the path, the node simply forwards the received data without any processing. Figure 2.1 shows a sensor network over a rectangular region of observation $\mathcal{R}$ with three base stations.

2.1.2 Node Energy Behaviour

Each node has a sensor, analog pre-conditioning and data conversion circuitry (A/D), digital signal processing and a radio link [66],[33]. The key energy parameters are the energies needed to i) sense a bit (E_{sense}), ii) receive a bit (E_{rx}), and iii) transmit a bit over a distance d, (E_{tx}). Assuming a d^{η} path loss model where η is the path loss
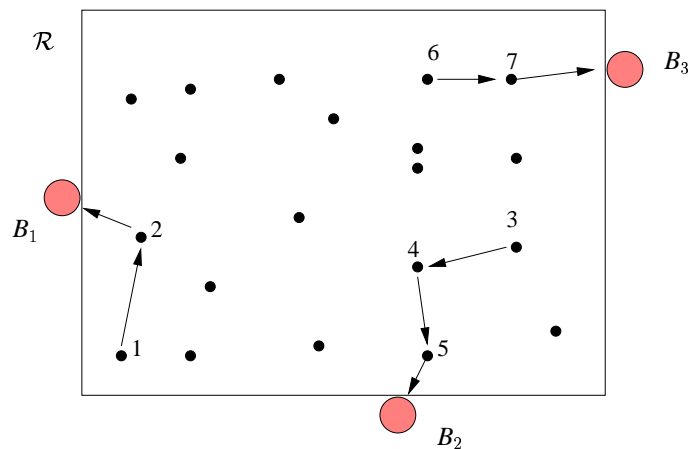
Figure 2.1: A sensor network over a rectangular region of observation $\mathcal{R}$ with three base stations B_1, B_2, B_3. Node 1 sends its data to base station B_1 via node 2. Node 3 sends its data to B_2 via nodes 4 and 5. Node 6 sends its data to B_3 via node 7.

exponent [67]

$$E_{tx} = \alpha_{11} + \alpha_2 d^\eta, \quad E_{rx} = \alpha_{12}, \quad E_{sense} = \alpha_3, \tag{2.1}$$

where α_{11} is the energy/bit consumed by the transmitter electronics, α_{12} is the energy/bit consumed by the receiver electronics, α_2 accounts for energy/bit dissipated in the transmit amplifier, and α_3 is the energy cost of sensing a bit [33]. Typically E_{sense} is much small compared to E_{tx} and E_{rx}. The energy/bit consumed by a node acting as a relay that receives data and then transmits it d meters onward is

$$E_{\text{relay}}(d) \;=\; \alpha_{11} + \alpha_2 d^\eta + \alpha_{12} \;=\; \alpha_1 + \alpha_2 d^\eta. \tag{2.2}$$

where $\alpha_1 = \alpha_{11} + \alpha_{12}$. If r is the number of bits relayed per second, then energy consumed per second (i.e., power) is given by

$$P_{\text{relay}}(d) = r \cdot E_{\text{relay}}(d). \tag{2.3}$$

We will use the following values for the energy parameters which are reported in the literature [68],[33]: $\alpha_1 = 180 \, \text{nJ/bit}$ and $\alpha_2 = 10 \text{pJ/bit}/m^2$ (for $\eta = 2$) or $0.001 \text{pJ/bit}/m^4$

(for $\eta = 4$).

2.1.3   Battery and Network Life

Each sensor node is powered by a finite-energy battery with an available energy of E_{battery} J at the initial network deployment. A sensor node ceases to operate if its battery is drained below a certain energy threshold (i.e., available energy goes below some usable threshold). Often, network lifetime is defined as the time for the first node to die [8],[9],[15],[33],[36] or as the time for a certain percentage of network nodes to die [21]. As in the above references, we define network lifetime as the time for the first node to die.

Given the region of observation ($\mathcal{R}$), number of nodes (N), initial energy in each node (E_{battery}), node energy parameters ($\alpha_1, \alpha_2, \alpha_3$), path loss parameters (η), we are interested in i) deriving bounds on the network lifetime when K, $K \geq 1$ base stations are deployed as data sinks along the periphery of the observation region, and ii) obtaining optimal locations of the base station.

2.1.4   Minimum Energy Relay Theorem

The bounding of network lifetimes often involves the problem of establishing a data link of certain rate r between a transmitter (A) and a receiver (B) separated by distance D meters. This can be done either by directly transmitting from A to B (single hop) or by using several intermediate nodes acting as relays (multihop). A scheme that transports data between two nodes such that the overall rate of energy dissipation is minimized is called a *minimum energy relay* [33]. If $M - 1$ relays are introduced between A and B, i.e., M links between A and B (see Fig. 2.2), the overall rate of dissipation is given by

$$P_{\text{link}}(D) = \sum_{i=1}^{M} P_{\text{relay}}(d_i) - \alpha_{12}, \tag{2.4}$$

where d_i is the inter-node distance of the ith link. The following minimum energy relay theorem in [33] is relevant in the lifetime derivation for multiple base stations scenario.
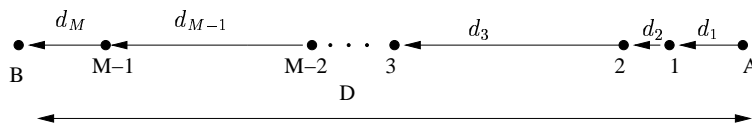
Figure 2.2: $M - 1$ relay nodes between points A and B.

Theorem: Given D and the number of intermediate relays $(M - 1)$, $P_{link}(D)$ is minimized when all hop distances (i.e., d_i's) are made equal to D/M.

From the above and (2.4), it can be seen that the optimum number of hops (links) is the one that minimizes $MP_{\text{relay}}(D/M)$, and is given by

$$M_{opt} = \left\lfloor \frac{D}{d_{\text{char}}} \right\rfloor \quad \text{or} \quad \left\lceil \frac{D}{d_{\text{char}}} \right\rceil, \tag{2.5}$$

where the distance d_{char}, called the characteristic distance, is independent of D and is given by

$$d_{\text{char}} = \sqrt[\eta]{\frac{\alpha_1}{\alpha_2(\eta - 1)}}. \tag{2.6}$$

That is, for a given distance D, there is an optimum number of relay nodes $(M_{opt} - 1)$; using more or less than this optimal number leads to energy inefficiencies. The energy dissipation rate of relaying a bit over distance D can be bounded as

$$P_{\text{link}}(D) \geq \left(\alpha_1 \frac{\eta}{\eta - 1} \frac{D}{d_{\text{char}}} - \alpha_{12} \right) r \tag{2.7}$$

with equality if and only if D is an integral multiple of d_{char}. From the minimum energy relay argument above, the actual power dissipated in the network is always larger than or equal to the sum of this $P_{\text{link}}(D)$ and the power for sensing, i.e.,

$$
\begin{aligned}
P_{\text{nw}} &\geq P_{\text{link}}(D) + P_{sense} \\
&\geq \left(\alpha_1 \frac{\eta}{\eta - 1} \frac{D}{d_{\text{char}}} - \alpha 12 \right) r + \alpha_3 r.
\end{aligned} \tag{2.8}
$$

As an approximation, the sensing power can be ignored since the power for relaying data

a) B_1 located on W-side

b) B_1 located on L-side
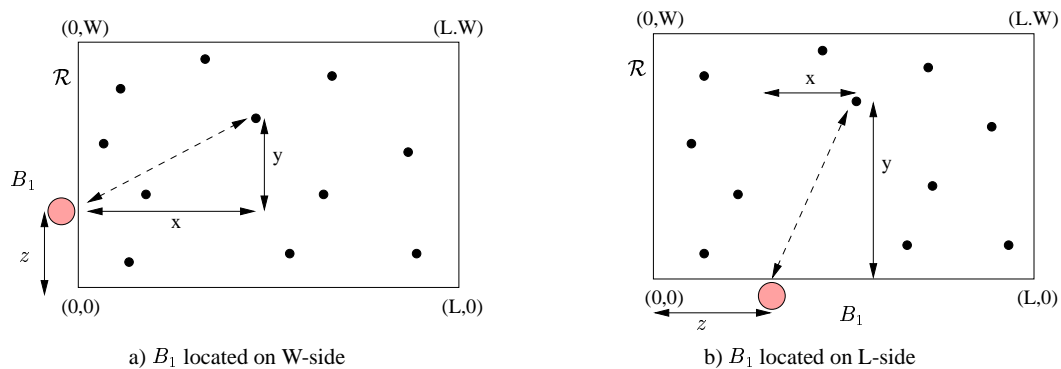
Figure 2.3: Single base station placements. a) B_1 located on W-side. b) B_1 located on L-side.

dominates.

2.2 Bounds on Network Lifetime

In this section, we derive upper bounds on the average lifetime of the network with multiple base stations. Consider a rectangular region of observation $\mathcal{R}$ with sensor nodes uniformly distributed in $\mathcal{R}$.

2.2.1 Single Base Station

Consider first the case of a single base station which is located on any one of the four sides of $\mathcal{R}$. Let the base station B_1 be located at a distance of z from the origin on the y-axis as shown in Fig. 2.3(a). Consider a source node in $\mathcal{R}$ at a distance of $D' = \sqrt{x^2 + y^2}$ from B_1. Denoting the energy dissipation in the entire network for a given base station location z by $P_{\mathrm{NW}}^{(z)}$, and assuming uniform distribution of N nodes, we have

$$P_{\mathrm{NW}}^{(z)} = N \int \int_{\mathcal{R}} P_{\mathrm{nw}}(x, y) \frac{1}{WL} \, dx \, dy. \tag{2.9}$$

By the minimum energy relay argument, it is seen that $P_{\mathrm{nw}}(x, y) \geq P_{\mathrm{link}}\left(\sqrt{x^2 + y^2}\right)$,

and hence

$$
\begin{aligned}
P_{\text{NW}}^{(z)} \; &\geq \; \frac{N}{WL} \int_{-z}^{W-z} \int_0^L P_{\text{link}} \left(\sqrt{x^2 + y^2} \right) dx \, dy \\
&\geq \; r\alpha_1 \frac{\eta}{\eta-1} \frac{N}{WL} \int_{-z}^{W-z} \int_0^L \frac{\sqrt{x^2 + y^2}}{d_{\text{char}}} dx \, dy \\
&\geq \; r\alpha_1 \frac{\eta}{\eta-1} \frac{d_{\text{one-BS}}(z)}{d_{\text{char}}},
\end{aligned}
\tag{2.10}
$$

where

$$
\begin{aligned}
d_{\text{one-BS}}(z) \; &= \; \frac{N}{WL} \int_{-z}^{W-z} \int_0^L \sqrt{x^2 + y^2} \, dx \, dy \\
&= \; \frac{N}{12WL} \Bigg(4Lz\sqrt{L^2 + z^2} + 4L(W-z)\sqrt{L^2 + (W-z)^2} \\
&\quad - (W-z)^3 \ln \left[\frac{(W-z)^2}{(L + \sqrt{L^2 + (W-z)^2})^2} \right] - z^3 \ln \left[\frac{z^2}{(L^2 + \sqrt{L^2 + z^2})^2} \right] \\
&\quad + 2L^3 \ln \left[W - z + \sqrt{L^+(W-z)^2} \right] \Bigg).
\end{aligned}
\tag{2.11}
$$

Achieving network lifetime demands that the total energy consumed in the network (P_{nw}) to be no greater than the total energy in the network at the beginning (NE_{battery}). Therefore, denoting $\mathcal{T}_{\text{one-BS}}^{(z)}$ as the network lifetime with one base station at a given location z, we have

$$
P_{\text{NW}}^{(z)} \, \mathcal{T}_{\text{one-BS}}^{(z)} \; \leq \; NE_{\text{battery}}.
\tag{2.12}
$$

An upper bound on the network lifetime for a given base station location z is then given by

$$
\mathcal{T}_{\text{one-BS}}^{(z)} \; \leq \; \frac{NE_{\text{battery}}}{r\alpha_1 \frac{\eta}{\eta-1} \frac{d_{\text{one-BS}}(z)}{d_{\text{char}}}}.
\tag{2.13}
$$

Now, optimal placement of the base station on the W-side in Fig. 2.3(a) can be obtained by choosing the z that maximizes the lifetime bound in (2.13), i.e.,

$$
z_{\text{opt}}^{(W)} \; = \; \underset{z \in (0, W)}{\text{argmax}} \; \mathcal{T}_{\text{one-BS}}^{(z)}.
\tag{2.14}
$$
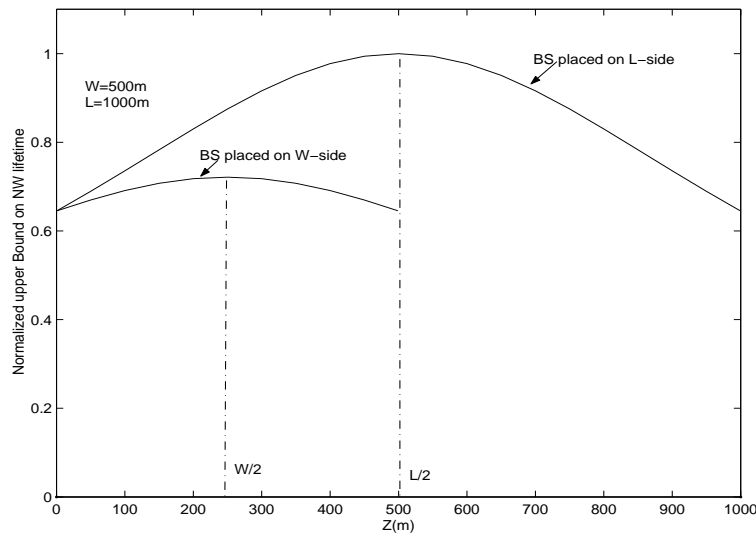
Figure 2.4: Normalized upper bound on network life time as a function of base station location for $L = 1000$ m and $W = 500$ m.

Maximizing (2.13) w.r.to z, we obtain the optimal base station location as

$$z_{opt}^{(W)} = W/2, \tag{2.15}$$

and substituting $z_{opt}^{(W)} = W/2$ in (2.11) gives a closed-form expression for $d_{\text{one-BS}}(z)$, which when substituted in (2.13) gives a closed-form expression for lifetime upper bound.

In a similar way, the optimal base station location and the corresponding lifetime bound can be obtained for the base station placement on the L-side as shown in Fig. 2.3(b), as

$$z_{opt}^{(L)} = L/2, \tag{2.16}$$

and the corresponding lifetime bound is obtained by simply interchanging W and L in the lifetime bound equation. It is seen that the for $L > W$, the optimal base station location is the midpoint of the L-side, and for $L \leq W$ the optimal location is the midpoint of the W-side. A numerical example illustrating this observation is shown in Fig. 2.4 for $L = 1000$ m, $W = 500$ m, and $E_{\text{battery}} = 0.05$ J.

2.2.2   Two Base Stations

Next, consider the case of two base stations where the base stations B_1 and B_2 can be deployed in such a way that:

1. *Same side orientation (SSO):* Both BSs are on the same side as shown in Fig. 2.5 (a). There are four such possibilities (i.e., both BSs can be deployed on any one of the four sides).

2. *Adjacent side orientation (ASO):* One BS each on adjacent sides as in Fig. 2.5 (b). There are four such possibilities.

3. *Opposite side orientation (OSO):* One BS each on opposite sides as in Fig. 2.5 (c). There are two such possibilities.

It is noted that, in order to jointly optimize the locations of B_1 and B_2, the network lifetime bounds for all the above possibilities of base station placement need to be derived. Due to the symmetry involved in the rectangular region considered, one possibility for each orientation needs new derivation. Accordingly, in the following, we present the derivation for the three different orientations shown in Figs. 2.5 (a), (b), and (c). Derivation for other possibilities follow similarly due to symmetry.

Each node in the network must be associated with any one base station. For each node, this can be done by choosing that base station towards which energy spent for delivering data from that node is minimum. From the minimum energy relay argument, the minimum energy spent is proportional to the distance D between source node and the base station (see RHS of Eqn. (2.7)), and hence associating the node to its closest base station results in the least minimum energy spent. Accordingly, we associate each node with its closest base station. This results in the region $\mathcal{R}$ to be partitioned into two sub-regions $\mathcal{R}_1$ and $\mathcal{R}_2$ such that all nodes in sub-region $\mathcal{R}_1$ will be nearer to B_1 than B_2, and all nodes in sub-region $\mathcal{R}_2$ will be nearer to B_2 than B_1. It can be seen that this partitioning will occur along the perpendicular bisector of the line joining B_1 and B_2.
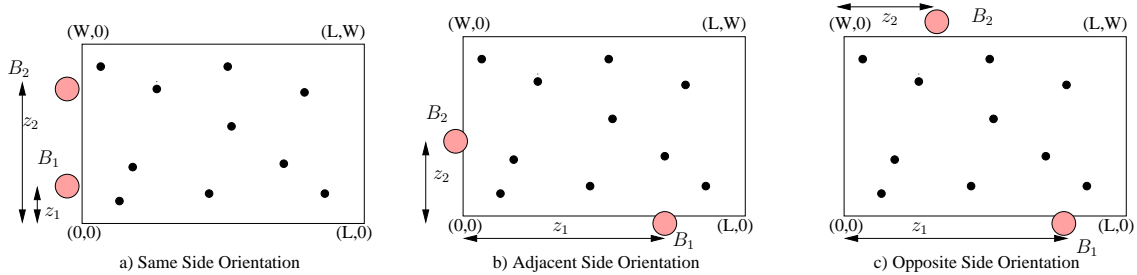
Figure 2.5: Placements of two base stations. a) Same side orientation, b) adjacent side orientation, and c) opposite side orientation.

Derivation for Adjacent Side Orientation (ASO)

We first consider the derivation of network lifetime bound for the case of adjacent side orientation shown in Fig. 2.5 (b), where B_1 is located on the x-axis at a distance of z_1 from the origin and B_2 is located on the y-axis at a distance of z_2 from the origin. The axis along which $\mathcal{R}_1$, $\mathcal{R}_2$ partition occurs depends on the locations of B_1 and B_2 (i.e., z_1 and z_2 in this case). For a given z_1 and z_2, the partition axis will belong to any one of the four possible axis types $X_a X_b$, $X_a Y_b$, $Y_a X_b$ and $Y_a Y_b$ as shown in Figs. 2.6 (a), (b), (c) and (d). The partition axis can be represented by the straight line

$$Y = mX + c, \tag{2.17}$$

where $m = \frac{z_1}{z_2}$ and $c = \frac{z_2^2 - z_1^2}{2z_2}$. Then, from (2.17) we have

$$X_a = X|_{Y=0} \implies X_a = -\frac{c}{m} = \frac{z_1^2 - z_2^2}{2z_1}, \tag{2.18}$$

$$X_b = X|_{Y=W} \implies X_b = \frac{W - c}{m} = \frac{W z_2}{z_1} - \frac{z_2^2 - z_1^2}{2z_1}, \tag{2.19}$$

$$Y_a = Y|_{X=0} \implies Y_a = c = \frac{z_2^2 - z_1^2}{2z_2}, \tag{2.20}$$

$$Y_b = Y|_{X=L} \implies Y_b = mL + c = \frac{L z_1}{z_2} + \frac{z_2^2 - z_1^2}{2z_2}. \tag{2.21}$$
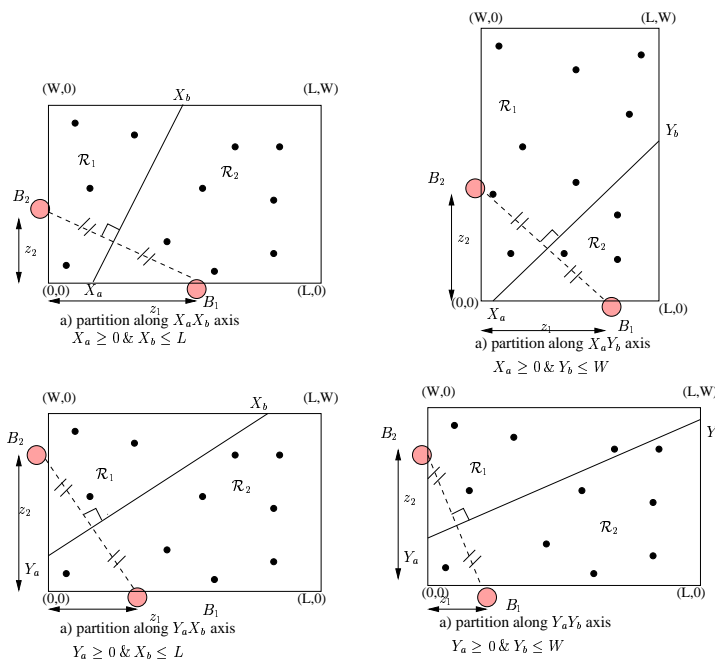
Figure 2.6: Adjacent side orientation of two base stations. $\mathcal{R}_1$, $\mathcal{R}_2$ partition can occur along a) $X_a X_b$ axis, b) $X_a Y_b$ axis, c) $Y_a X_b$ axis, and d) $Y_a Y_b$ axis.

It is noted that for a given z_1 and z_2, the partition axis type is

i) $X_a X_b$ if $X_a \geq 0$ and $X_b \leq L$ (Fig. 2.6(a)),

ii) $X_a Y_b$ if $X_a \geq 0$ and $Y_b \leq W$ (Fig. 2.6(b)),

iii) $Y_a X_b$ if $Y_a \geq 0$ and $X_b \leq L$ (Fig. 2.6(c)), and

iv) $Y_a Y_b$ if $Y_a \geq 0$ and $Y_b \leq W$ (Fig. 2.6(d)).

Now the energy dissipation in the entire network with base station locations z_1 and z_2 for the ASO case is given by

$$P_{\text{NW,aso}}^{(z_1,z_2)} \;=\; N \left(\int\!\!\int_{\mathcal{R}_1} P_{\text{nw}}(x,y) \, \frac{1}{WL} \, dx\,dy + \int\!\!\int_{\mathcal{R}_2} P_{\text{nw}}(x,y) \, \frac{1}{WL} \, dx\,dy \right). (2.22)$$

By minimum energy relay argument, $P_{\text{nw}}(x, y) \geq P_{\text{link}}\left(\sqrt{x^2 + y^2}\right)$, and hence

$$
\begin{aligned}
P_{\text{NW,aso}}^{(z_1, z_2)} &\geq \frac{N}{WL} \left(\int\int_{\mathcal{R}_1} P_{\text{link}}\left(\sqrt{x^2 + y^2}\right) dx\, dy + \int\int_{\mathcal{R}_2} P_{\text{link}}\left(\sqrt{x^2 + y^2}\right) dx\, dy \right) \\
&\geq \frac{r\alpha_1}{d_{\text{char}}} \frac{\eta}{\eta - 1} \frac{N}{WL} \left(\int\int_{\mathcal{R}_1} \sqrt{x^2 + y^2}\, dx\, dy + \int\int_{\mathcal{R}_2} \sqrt{x^2 + y^2}\, dx\, dy \right) \\
&\geq \frac{r\alpha_1}{d_{\text{char}}} \frac{\eta}{\eta - 1} \frac{N}{WL} \left(d_{\text{2-BS,aso}}^{\mathcal{R}_1}(z_1, z_2) + d_{\text{2-BS,aso}}^{\mathcal{R}_2}(z_1, z_2) \right),
\end{aligned}
\tag{2.23}
$$

where $d_{\text{2-BS,aso}}^{\mathcal{R}_1}(z_1, z_2)$ and $d_{\text{2-BS,aso}}^{\mathcal{R}_2}(z_1, z_2)$ are different for different partition axis types, and are of the form

$$
d_{\text{2-BS,aso}}^{\mathcal{R}_1}(z_1, z_2) = \int_{y_1}^{y_2} \int_{x_1}^{x_2} \sqrt{x^2 + y^2}\, dx\, dy + \int_{y_3}^{y_4} \int_{x_3}^{x_4} \sqrt{x^2 + y^2}\, dx\, dy, \tag{2.24}
$$

and

$$
d_{\text{2-BS,aso}}^{\mathcal{R}_2}(z_1, z_2) = \int_{x_5}^{x_6} \int_{y_5}^{y_6} \sqrt{x^2 + y^2}\, dy\, dx + \int_{x_7}^{x_8} \int_{y_7}^{y_8} \sqrt{x^2 + y^2}\, dy\, dx. \tag{2.25}
$$

Defining $X_{z_2} = X|_{Y = y + z_2}$ and $Y_{z_1} = Y|_{X = x + z_1}$ in (2.17), the values of the limits $y_1, y_2, \cdots, y_8$ and $x_1, x_2, \cdots, x_8$ in (2.24) and (2.25) for the various partition axis types in Figs. 2.6 (a), (b), (c), and (d) are tabulated in Table 2.1.

Now, denoting $\mathcal{T}_{\text{2-BS,aso}}^{(z_1, z_2)}$ as the network lifetime with two base stations at locations z_1, z_2 for the ASO case, we have

$$
P_{\text{NW,aso}}^{(z_1, z_2)}\, \mathcal{T}_{\text{2-BS,aso}}^{(z_1, z_2)} \leq N E_{\text{battery}}, \tag{2.26}
$$

and hence an upper bound on lifetime for a given z_1 and z_2 and ASO can be obtained as

$$
\mathcal{T}_{\text{2-BS,aso}}^{(z_1, z_2)} \leq \frac{N E_{\text{battery}}}{\frac{r\alpha_1}{d_{\text{char}}} \frac{\eta}{\eta - 1} \frac{N}{WL} \left(d_{\text{2-BS,aso}}^{\mathcal{R}_1}(z_1, z_2) + d_{\text{2-BS,aso}}^{\mathcal{R}_2}(z_1, z_2) \right)}. \tag{2.27}
$$

The optimum base station locations for ASO case that maximizes the above lifetime

Limits	For X_aX_b axis Fig.2.6(a)	For X_aY_b axis Fig.2.6(b)	For Y_aX_b axis Fig.2.6(c)	For Y_aY_b axis Fig.2.6(d)
(x_1, x_2)	$(0, X_{z_2})$	$(0, X_{z_2})$	$(0, X_{z_2})$	$(0, X_{z_2})$
(y_1, y_2)	$(-z_2, W - z_2)$	$(-z_2, Y_b - z_2)$	$(Y_a - z_2, Y_b - z_2)$	$(Y_a - z_2, W - z_2)$
(x_3, x_4)	$(0, 0)$	$(0, L)$	$(0, L)$	$(0, 0)$
(y_3, y_4)	$(0, 0)$	$(Y_b - z_2, W - z_2)$	$(Y_b - z_2, W - z_2)$	$(0, 0)$
(x_5, x_6)	$(X_a - z_1, X_b - z_1)$	$(X_a - z_1, L - z_1)$	$(-z_1, L - z_1)$	$(-z_1, X_b - z_1)$
(y_5, y_6)	$(0, Y_{z_1})$	$(0, Y_{z_1})$	$(0, Y_{z_1})$	$(0, Y_{z_1})$
(x_7, x_8)	$(X_b - z_1, L - z_1)$	$(0, 0)$	$(0, 0)$	$(X_b - z_1, L - z_1)$
(y_7, y_8)	$(0, W)$	$(0, 0)$	$(0, 0)$	$(0, W)$

Table 2.1: Limits $y_1, y_2, \cdots, y_8$ and $x_1, x_2, \cdots, x_8$ in (2.24) and (2.25) for two base station ASO for various partition axis types in Figs. 2.6 (a), (b), (c), and (d).

bound is then given by

$$\left(z_{1,\text{opt}}, z_{2,\text{opt}}\right)_{\text{aso}} = \underset{\substack{z_1 \in (0,L), \\ z_2 \in (0, W)}}{\text{argmax}} \ \mathcal{T}_{\text{2-BS,aso}}^{(z_1,z_2)}. \tag{2.28}$$

Following similar steps, the lifetime bounds for the cases SSO and OSO, $\mathcal{T}_{\text{2-BS,sso}}^{(z_1,z_2)}$ and $\mathcal{T}_{\text{2-BS,oso}}^{(z_1,z_2)}$, respectively, can be derived. These derivations are presented in Appendix A.

Finally, the optimum locations of the base stations are chosen from the best locations of ASO, SSO and OSO cases, as

$$\left(z_{1,\text{opt}}, z_{2,\text{opt}}\right) = \underset{\substack{z_1 \in (0,L), \\ z_2 \in (0,W) \\ \text{orient} \in \{\text{aso,sso,oso}\}}}{\text{argmax}} \ \mathcal{T}_{\text{2-BS,orient}}^{(z_1,z_2)}. \tag{2.29}$$

Two Base Stations (Jointly Optimum)			
Orientation		NW life time Upper Bound (# rounds)	Optimal locations of B_1, B_2
SSO	W side	18.28	$(0, 121.3), (0, 381.5)$
	L side	31.36	$(133.7, 0), (761.4, 0)$
ASO		32.60	$(693.2, 0), (0, 263.6)$
OSO	W side	31.41	$(0, 249.4), (1000, 251.2)$
	L side	32.99	$(716.6, 0), (500, 282.6)$

Table 2.2: Upper bounds on network lifetime and optimal base station locations. Two base stations. Joint optimization. $L = 1000$ m, $W = 500$ m.

Numerical Results for Two Base Stations

We carried out the optimization of (2.28) using genetic algorithm and obtained the network lifetime[1] upper bound and the optimum base station locations. The results thus obtained for SSO, ASO, and OSO cases are given in Table 2.2 for $L = 1000$ m, $W = 500$ m, and $E_{battery} = 0.5$ J. From the above results, it can be observed that the maximum lifetime bound occurs when the base stations are placed with opposite side orientation (OSO) on the L-side, and the corresponding coordinates of the optimum locations of B_1 and B_2 are (716.6 m, 0 m) and (500 m, 282.6 m). Thus, given the region of observation (in terms of W and L), initial battery energy (E_{battery}), path loss characteristics (η), and energy consumption behaviour of the node electronics (α_1, α_2), the above analysis allows us to compute an upper bound on the network lifetime and the corresponding optimum base station locations for the two base stations case.

2.2.3   Jointly Optimum vs Individually Optimum

It is noted that in the above optimization procedure, the locations of B_1 and B_2 are jointly optimized. Though such joint optimization is best in terms of performance, its complexity is high. Also, such joint optimization will become prohibitively complex for more number

---

[1]We present the network lifetime in terms of number of rounds where one round = 2000 secs. Same definition is adopted in the simulation results in Sec. 2.3 also.

Two Base Stations (Individually Optimum)		
Location of B_1 fixed at $(L/2, 0) = (500, 0)$		
Orientation	NW life time Upper Bound (# rounds)	Optimal location of B_2
SSO	28.36	$(164.9, 0)$
ASO	30.22	$(0, 496.2)$
OSO	31.41	$(502.5, 500)$

Table 2.3: Upper bounds on network lifetime and optimum base station locations for two base stations. B_1 fixed at optimum location obtained from solving single BS problem. $L = 1000$ m, $W = 500$ m.

of base stations. So, an alternate and relatively less complex solution is to individually optimize B_1 and B_2, i.e., fix the location of B_1 at the optimal location obtained from the solution of the one base station problem and find the optimal location for B_2 and the corresponding lifetime bound. We carried out such an individual optimization for two base stations (by fixing BS B_1 at its individually optimum location $(L/2, 0)$), and the results of the optimization are given in Table 2.3. From Table 2.3, it can be observed that, as expected, the individually optimized solution results in reduced lifetime bound compared to the jointly optimized solution (e.g., 31.41 rounds vs 32.99 rounds for OSO). However, the individually optimized approach has the advantage of being attractive for solving the problem with more number of base stations. Like the jointly optimized solution, the individually optimized solution also results in the largest lifetime bound when the two base stations are deployed with opposite side orientation (OSO) on the L-side.

2.2.4   Three Base Stations

As pointed out earlier, for the case of three base stations, jointly optimizing the locations of B_1, B_2, B_3 can be prohibitively complex. Hence, in solving the three base stations problem, we take the approach of fixing the previously optimized locations of B_1, B_2 obtained from the solution of two base station problem, and then optimize the location
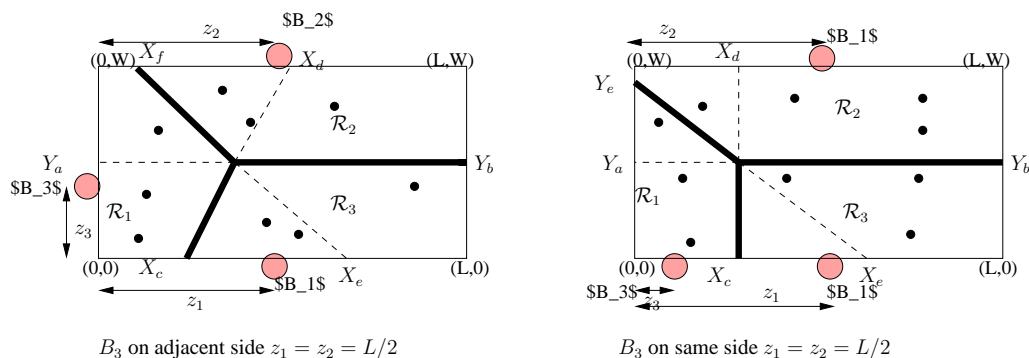
Figure 2.7: Placement of three base stations. B_1 and B_2 are placed at optimal locations obtained by solving the two base station problem. Location of B_3 is then optimized. a) B_3 on same side as B_1. b) B_3 on adjacent side of B_1.

of B_3. Once the base stations B_1 and B_2 are fixed, the problem gets simplified to optimizing only over B_3 location.

Fixing B_1 and B_2 on the midpoints of opposite sides (which is the individually optimum two BS solution), B_3 can be located on any one of four sides. Placement of B_3 with adjacent side orientation (ASO) and same side orientation (SSO) as shown in Figs. 2.7 (a) and (b), respectively, need to be considered separately. In each of these AS and SS orientation possibilities, the region $\mathcal{R}$ is partitioned into sub-regions $\mathcal{R}_1$, $\mathcal{R}_2$, and $\mathcal{R}_3$. The partition occurs along the three axes which are the perpendicular bisectors of the lines connecting the three different BS pairs as shown in Figs. 2.7(a) and (b). Proceeding in a similar way as done for the two BS problem, we have derived expressions for the upper bound on the network lifetime with three base stations. The derivation is given in Appendix B. These expressions were then optimized using genetic algorithm to compute the lifetime upper bound as well as the optimum location of B_3.

Table 2.2.4 shows the upper bound on the network lifetime computed for a) SS orientation and b) AS orientation. It can be seen that the AS orientation of B_3 results in a larger lifetime bound compared to SS orientation. The maximum lifetime bound for ASO is 38.38 rounds and the optimum location at which this maximum occurs is $(0, 249.8)$.

Three Base Stations (Individually Optimum)		
Location of B_1 fixed at (500,0)		
Location of B_2 fixed at (500,500)		
Orientation	NW life time Upper Bound (# rounds)	Optimum location of B_3
SSO	36.44	$(152.6, 0)$
ASO	38.38	$(0, 249.8)$

Table 2.4: Upper bounds on network lifetime and optimum base station locations for three base stations. B_1 and B_2 fixed at optimum locations obtained from solving two base stations problem. $L = 1000$ m. $W = 500$ m.

In Table 2.5, we present a comparison between the network lifetime bounds for one, two, and three base stations and their corresponding optimum BS locations. From Table 2.5, it can be observed that the lifetime bound increases for increasing number of base stations, as expected. For example, the lifetime bound is 24.3 rounds for one base station, whereas it gets increased to 38.4 rounds when three base stations are employed.

No. of BS	NW life time Upper Bound (# rounds)	Optimum BS Locations
One BS	24.34	$B_1 : (489.9, 0)$
Two BS (Jointly opt)	32.99	$B_1 : (716.6, 0)$, $B_2 : (500, 282.6)$
Two BS (Indiv. opt)	31.41	$B_1 : (500, 0)$, $B_2 : (502.5, 500)$
Three BS (Indiv. opt)	38.38	$B_1 : (500, 0)$, $B_2 : (500, 500)$ $B_3 : (0, 249.8)$

Table 2.5: Comparison of the upper bounds on network lifetime for one, two, and three base stations. $L = 1000$ m, $W = 500$ m.

2.3   Simulation Results

In order to validate the analytical bound on the network life time, we carried out detailed simulations and obtained the simulated network lifetime over several network realizations at different BS locations. In the simulations, 50 nodes are distributed uniformly in the rectangular region of observation $\mathcal{R}$ with $L = 1000$ m and $W = 500$ m. All nodes have an initial battery energy of 0.5 J. The Minimum cost forwarding (MCF) routing protocol in [25] is employed to route packets from nodes to their assigned base stations. At the media access control (MAC) level, Self-organizing Medium Access Control for Sensor networks (SMACS), a contention-free MAC protocol presented in [27] is employed to provide channel access for all the nodes. Data packets are of equal length. Each packet has 200 bits. Time axis is divided in to rounds, where each round consists of 300 time frames. Each node generates 1 packet every 30 frames; i.e., 10 packets per round. For each network realization in the simulation, the number of rounds taken for the first node to die (i.e., network lifetime in number of rounds) is obtained. This lifetime averaged over several realizations of the network with 95 % confidence for different number and locations of the base stations are plotted in Figs. 2.8 to 2.10.

Figures 2.8, 2.9 and 2.10 compare the simulated network lifetime with the theoretical upper bound for one, two, and three base stations, respectively. In Fig. 2.8, the BS B_1 location is varied from (0,0) to (1000,0). The theoretical analysis predicted that the maximum lifetime bound occurs at $L/2$ (i.e., (500,0) in this case). The simulated lifetime also is maximum at the B_1 location of (500,0). Also, the simulated lifetime is less than the analytical upper bound. The gap between the simulated lifetime and the upper bound implies that better protocols can be devised to achieve lifetimes closer to the bound. For the two base stations scenario in Fig. 2.9, B_1 is fixed at (500,0) and the B_2 location is varied from (500,0) to (500,1000). Analytical prediction is that optimum B_2 location is (500,500). It is interesting to see that in the simulation also maximum network lifetime occurs when B_2 is located at (500,500). In addition, for the two base stations case, the protocols employed in the simulations are found to achieve lifetimes close to the upper bound. A similar observation can be made from Fig. 2.10 for the
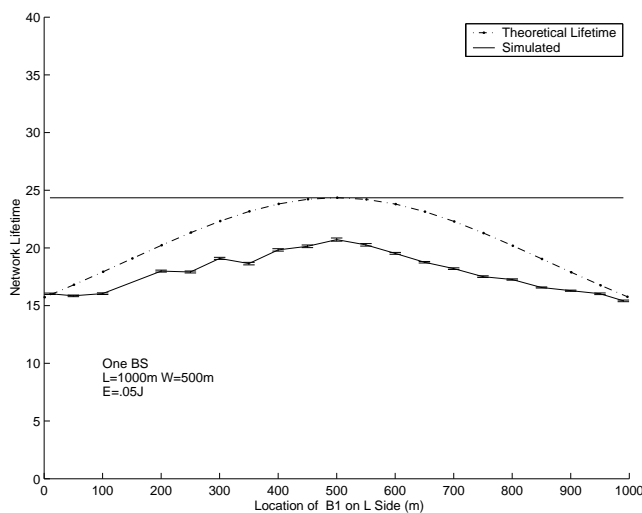
Figure 2.8: Comparison of simulated network life time with theoretical upper bound for single base station case. $L = 1000$ m, $W = 500$ m, $E_{\text{battery}} = 0.5$ J. Location of B_1 varied from (0,0) to (1000,0).

three base stations case as well. In summary, the simulations validate the analytical lifetime bounds derived, and also corroborate the expected result that network lifetime can be increased by the use of multiple base stations, and more so when their locations are chosen optimally as our study/results clearly illustrate.

2.4   Conclusions

We addressed the fundamental question concerning the limits on the network lifetime in sensor networks with multiple base stations. We derived upper bounds on the network lifetime when multiple base stations are employed. We also obtained optimum locations of the base stations that maximize these network lifetime bounds. For a scenario with single base station and a rectangular region of observation, we obtained closed-form expressions for the network lifetime bound and the optimum base station location. For the case of two base stations, we jointly optimized the base station locations by maximizing the lifetime bound using a genetic algorithm based optimization. Since joint optimization for more number of base stations is complex, for the case of three base stations, we
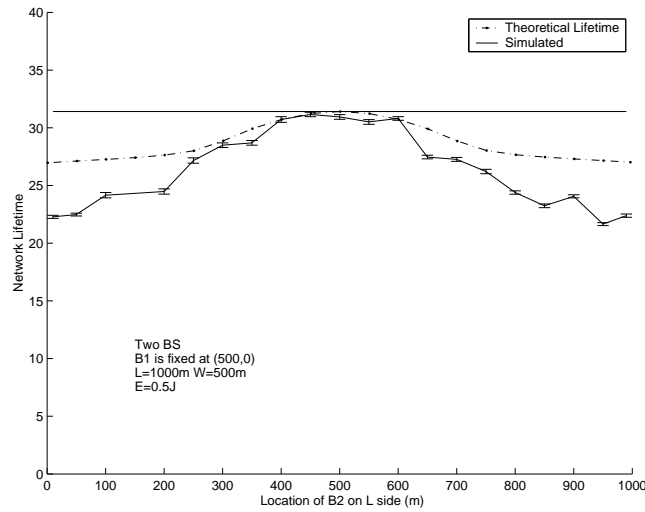
Figure 2.9: Comparison of simulated network lifetime with theoretical upper bound for two base stations. $L = 1000$ m, $W = 500$, $E_{\text{battery}} = 0.5$ J. B_1 fixed at $(500,0)$. Location of B_2 varied from $(0,500)$ to $(1000,500)$.
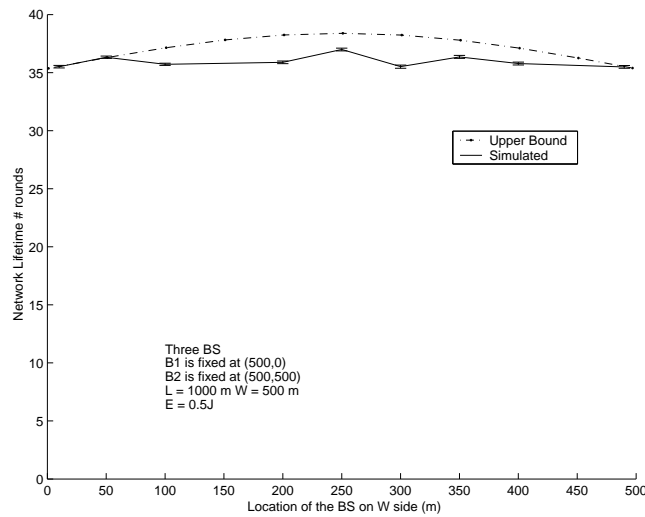
Figure 2.10: Comparison of simulated network lifetime with theoretical upper bound for three base stations. $L = 1000$ m, $W = 500$, $E_{\text{battery}} = 0.5$ J. B_1 fixed at $(500,0)$. B_2 fixed at $(500, 500)$. Location of B_3 varied from $(0,0)$ to $(0,500)$.

optimized the third base station location using the previously obtained optimum locations of the first two base stations. We provided simulation results that validated the network lifetime bounds and the optimal choice of the locations of the base stations.

Chapter 3

Base Stations Placement Problem

In this chapter, we investigate Moving base stations (BSs) approach described in Sec.1.3.2 by considering the following system model. Instead of allowing the BSs to go near the sensor nodes (due to, for example, the sensing area being hostile/inaccessible), the BSs are allowed to dynamically change their locations chosen from a set of *feasible BS locations* (refer to them as 'feasible sites') along the boundary of the sensing area. Suppose there are K, $K \geq 1$ BSs, and N, $N > K$ feasible sites. The problem to solve is to dynamically choose the optimum locations for the K BSs from the N feasible sites that maximize the network lifetime.

We divide the time axis into *rounds* of equal period. Placement of base stations is carried out at the beginning of each round and held for the entire duration of the round. A new placement is carried out in the beginning of the next round, and so on, till the end of network life. In [32], the base stations placement problem is formulated as an optimization problem and the optimum base stations locations are obtained as the solution to an Integer Linear Program (ILP). The complexity of the ILP solution however is high. In this chapter, we propose energy efficient low-complexity algorithms to determine the base station locations; they include

1. Top-K_{max} algorithm,

2. maximizing the minimum residual energy (Max-Min-RE) algorithm, and

3. minimizing the residual energy difference (MinDiff-RE) algorithm.

We show that the above proposed base stations placement algorithms provide increased network lifetimes and amount of data delivered during the network lifetime compared to single base station scenario as well as multiple static mobile base stations scenario, and close to those obtained by solving an ILP to determine the locations of the mobile base stations. We also investigate the additional lifetime gain that can be achieved when an energy aware routing protocol is employed in a multiple base stations scenario.

The rest of this chapter is organized as follows. In Section 3.1, we present the system model. In Section 3.2, we present the proposed base stations placement algorithms. In Section 3.3, we present the performance results and discussions. Finally, conclusions are given in Section 3.4.

3.1   System Model

We consider the following system model and assumptions.

3.1.1   Network

A set of sensor nodes V_s are uniformly distributed over a square sensor field. A set of feasible sites V_f (i.e., feasible base station locations) along the periphery of the sensor field is assumed. The sensor network is then represented as a graph $G(V, E)$, where $V = V_s \cup V_f$, and $E \subseteq V \times V$ represents the set of wireless links. Wireless links between sensor nodes and a feasible site refer to the links that would exist if a base station is located at that particular site.

There are K, $K \geq 1$ base stations to deploy. Time is divided into *rounds* of equal period. Selection of base station locations from the set of feasible sites V_f is made at the beginning of each round, and the base stations are moved and placed in these chosen locations for the entire duration of that round. A new set of base station locations are

computed at the beginning of the next round (and the base stations moved to these newly chosen locations), and so on, till the end of network life.

3.1.2 Transceiver

The transmission range of all sensor nodes is same and fixed. As in similar system models in the literature [8, 9], the energy spent in transmitting a bit over a distance d is assumed to be proportional to d^2.

3.1.3 MAC and Routing

Data packets generated at each sensor node is assumed to be of equal length. Also, each sensor node is assumed to generate equal amount of data per unit time. At the media access control (MAC) level, Self-organizing Medium Access Control for Sensor networks (SMACS), a contention-free MAC protocol presented in [27] is employed to provide channel access for all the sensor nodes. For multi-hop routing, minimum cost forwarding (MCF) protocol presented in [25] is employed.

3.1.4 Battery and Network Life

Each sensor node is powered by a finite-energy battery with an available energy of $E_{battery}$ J at the initial network deployment. At the sensor node, transmission of a data packet consumes E_t J of energy, and reception of a data packet consumes E_r J. A sensor node ceases to operate if its battery is drained below a certain energy threshold (i.e., available energy goes below a certain threshold). End of network life is said to be reached either if the batteries of all the sensor nodes are drained below the threshold or if all the live sensor nodes are disconnected from all the feasible sites (i.e., if all live nodes remain beyond the connectivity range of all feasible sites).

With the above system model, we need to choose optimum base station locations from V_f at the beginning of each round. In the following section, we present efficient algorithms for this base station placement problem.

3.2 Base Stations Placement Algorithms

The base stations placement problem in the above system model has been formulated as an optimization problem in [32], and the optimum base station locations are obtained as the solution to an ILP. However, the complexity of the ILP solution is high. In this section, we propose three energy efficient low-complexity algorithms to solve the base stations placement (BSP) problem.

Let s_i denote the location of sensor node i, $i \in V_s$, and f_i denote the location of feasible site i, $i \in V_f$. Let r denote the transmission range of each sensor node. Let RE_i denote the residual battery energy in sensor node i at the beginning of a round when the base station locations are computed.

3.2.1 Top-K_{max} Algorithm

This algorithm selects those feasible sites (maximum K sites) whose nearest neighbour nodes have the highest residual energies. Since the first-hop neighbour node to a base station has to handle all the transit packets from other nodes towards that base station, it can drain its battery sooner. Therefore, by assigning the nearest neighbour with highest residual energy nodes to serve as the first-hop neighbour nodes in each round, the life of the nodes in the network and hence network lifetime can get extended. The algorithm works as follows.

1. For each feasible site $i \in V_f$, find the nearest sensor node n_i within the connectivity range r, i.e., for each $i \in V_f$ choose sensor node $n_i \in V_s$ such that

$$|f_i - s_{n_i}| \leq |f_i - s_j|, \ \forall \, j \in V_s, j \neq n_i. \tag{3.1}$$

and

$$|f_i - s_{n_i}| \leq r. \tag{3.2}$$

2. Order these nearest neighbour nodes $\{n_i, i \in V_f\}$ in descending order of their residual energies, RE_{n_i}.

3. Select a maximum of K nodes from the top in this ordered list, and declare their corresponding nearest feasible sites as the solution.

As can be seen, this is a greedy algorithm. A main advantage of this algorithm is its simplicity and less computation complexity. If n is the number of sensor nodes and N is the number of feasible sites, then the complexity of this algorithm is given by $nN + N \log N$, which is linear in n.

3.2.2   Max-Min-RE Algorithm

Since the Top-K_{max} solution in the above algorithm gives preference to nearest neighbour nodes, it is likely that the nodes nearer to the feasible sites are loaded heavily and their batteries drained sooner than other nodes. The following Max-Min-RE algorithm (maximizing the minimum residual energy algorithm) attempts to distribute the load more evenly to different nodes. The Max-Min-RE algorithm works as follows. There are N feasible sites and K base stations to deploy, $N \geq K$. The number of base stations placement solutions are $P = \binom{N}{K}$. Let this solution set be S. Let the jth solution in the solution set S be denoted by T_j.

1. Determine set $S_c \subseteq S$ such that $S_c = \{T_j : \forall i \in V_s$ there exists $p \in V_s$ such that $|s_i - s_p| \leq r$ or $q \in V_f$ such that $|s_i - f_q| \leq r\}$.

2. For a given solution $T_j \in S_c$, determine the routes from all the sensor nodes to their respective base stations using MCF routing.

3. For each node $i \in V_s$ compute the energy consumed at all nodes in the path in delivering a data packet from node i to its corresponding base station, and determine the resulting residual energies in all nodes.

4. Find the minimum residual energy among all nodes in the jth solution

$$M_j = \min_{i \in V_s}\{RE_i\}. \tag{3.3}$$

5. Choose the solution as

$$T_{Max-Min-RE} \; = \; \max_{j}\{M_j : T_j \in S_c\}. \tag{3.4}$$

By this algorithm, we are choosing that solution in which the heavily loaded node (identified by the minimum residual energy among various nodes in a given solution, and not by the minimum distance as done in the Top-K_{max} algorithm) has the maximum residual energy among all possible solutions. This algorithm hence is expected to distribute (and drain energy) evenly among the nodes without bias to nearest neighbour nodes. The algorithm results in a complexity of $P(Nn + Kn + an^2 + N\log N + \log P)$, i.e., since N, K and P are typically small compared to n, the algorithm has n^2 complexity.

3.2.3   MinDiff-RE Algorithm

In this algorithm, which we call as MinDiff-RE algorithm (minimizing the difference in residual energy algorithm), the idea again is to evenly drain the nodes. It is similar to the Max-Min-RE algorithm, except that we choose that solution for which the difference between the maximum and minimum residual energies in nodes is minimized (rather than maximizing the minimum residual energy as in Max-Min-RE algorithm. The MinDiff-RE algorithm works as follows.

1. Perform steps 1) to 3) of the Max-Min-RE algorithm.

2. Compute the metric

$$M_j \; = \; \max_{i \in V_s}\{RE_i\} \;\; - \;\; \min_{i \in V_s}\{RE_i\}. \tag{3.5}$$

3. Choose the solution as

$$T_{MinDiff-RE} = \min_{j}\{M_j : T_j \in S_c\}. \tag{3.6}$$
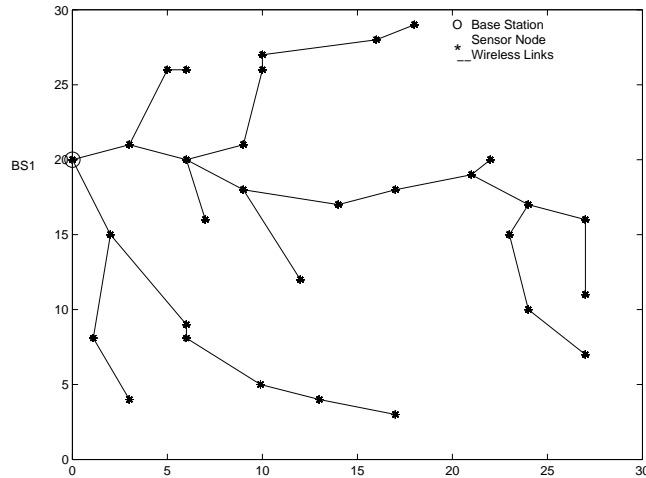
Figure 3.1: MCF routing in single base station scenario.

The complexity of this algorithm is same as that of the Max-Min-RE algorithm presented in Sec. 3.2.2.

3.3   Performance Results

We evaluated the performance of the above base stations placement (BSP) algorithms through simulations. The simulation model is as follows.

3.3.1   Simulation Model

A square sensor field of area 30 m $\times$ 30 m (Fig. 3.1) is considered. The number of sensor nodes in the network is 30. Sensor nodes are uniformly distributed in the network area. The number of feasible sites is taken to be 8, and the coordinates of these feasible sites are $\{(0, 10), (0, 20), (10, 30), (20, 30), (30, 20), (30, 10), (20, 0), (10, 0)\}$, as shown in Fig. 3.2. The maximum number of mobile base stations is taken to be 3 (i.e., $K = 3$). Each sensor node is provided with an initial energy of $E_{battery} = 0.05$ J. The transmission range of each sensor node is set to 10 meters. As in [8, 9], the energy spent in transmitting a bit over 1 meter distance is taken as $0.1nJ/bit - m^2$ [32],[8, 9] and the energy spent in
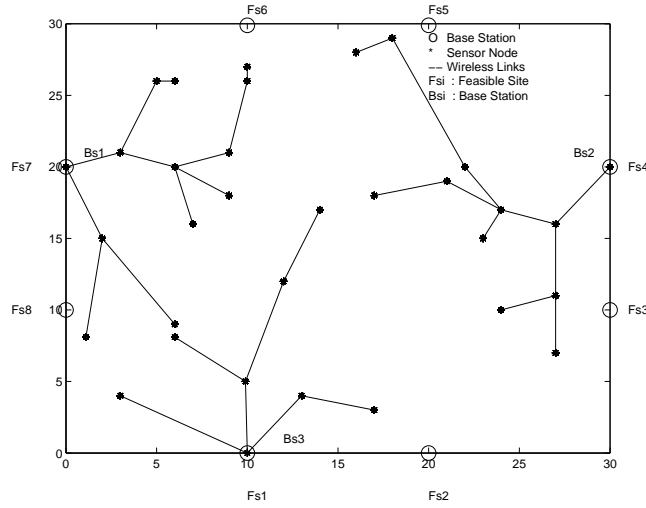
Figure 3.2: MCF routing in three base stations scenario.

receiving a bit is set to 50 nJ/bit. The packet length is fixed at 200 bits. Each round lasts 300 time frames. Each node generates 1 packet every 30 frames; i.e., each node generates 10 packets per round. The performance measures of interest are the network lifetime (as defined in Sec. 3.1.4) and the amount of data packets delivered during the lifetime of the network. We evaluate and compare the above performance measures for various BSP algorithms, including:

1. Single static base station

2. Three static base stations

3. Three mobile base stations, $\text{Top}_{K_{max}}$ algorithm

4. Three mobile base stations, Max-Min-RE algorithm

5. Three mobile base stations, MinDiff-RE algorithm

6. Three mobile base stations, ILP solution (this scheme is same as Scheme 4 in [32])

In scheme 1), only one base station is used in a fixed location (as shown in Fig. 3.1). In scheme 2, three base stations are used, but at fixed locations as shown in Fig. 3.2

(these locations are not changed from one round to the other). Schemes 3), 4) and 5) are the proposed Top-K_{max}, Max-Min-RE, and MinDiff-RE algorithms, respectively. The case of ILP solution in scheme 6) corresponds to the optimization problem formulation presented in [32], which is stated as below: Let y_l be a 0-1 integer variable for each $l \in V_f$ such that $y_l = 1$ if a base station is located at feasible site l; 0 otherwise. Defining $\mathcal{N}(i)$ to be the set of neighbours of node i, L to be the number of time frames per round, x_{ij} to be the number of packets node i transmits to j, $j \in \mathcal{N}(i)$, and $0 < \alpha \leq 1$, the solution $y_l, l \in V_f$ is obtained by solving the following ILP which minimizes the maximum energy spent, E_{max}, by a sensor node in a round

$$\text{Minimize} \quad E_{max}$$

such that

$$\sum_{j \in \mathcal{N}(i)} x_{ij} - \sum_{k \in \mathcal{N}(i)} x_{ki} = L, \ i \in V_s \tag{3.7}$$

$$E_t \sum_{j \in \mathcal{N}(i)} x_{ij} + Er \sum_{k \in \mathcal{N}(i)} x_{ki} \leq \alpha RE_i, \ i \in V \tag{3.8}$$

$$\sum_{l \in V_f} y_l \leq K \tag{3.9}$$

$$\sum_{i \in V_s} x_{ik} \leq L|V_s|y_k, \quad k \in V_f \tag{3.10}$$

$$E_t \sum_{j \in \mathcal{N}(i)} x_{ij} + E_r \sum_{k \in \mathcal{N}(i)} x_{ki} \leq E_{max}, \ i \in V \tag{3.11}$$

$$x_{ij} \geq 0, \ i \in V_s, \ j \in V; \quad y_k \in \{0, 1\}, \ k \in V_f. \tag{3.12}$$

We have used CPLEX (version 9) to solve the above ILP. As in [32], for each instance, the value of the parameter α was initially set to 0.2 and incremented in steps of 0.2 in case the instance was infeasible.
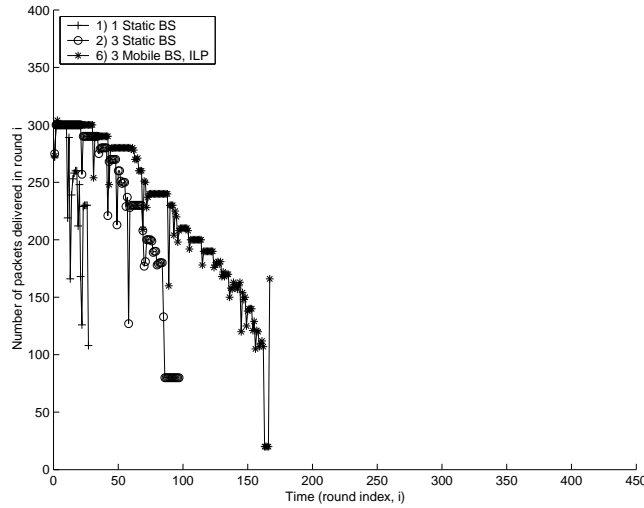
Figure 3.3: Traces of number of packets delivered per round as a function of time for schemes 1), 2), and 6). MCF routing. Initial energy at each node, $E_{battery} = 0.05$ J. One packet $= 200$ bits. Range of each node, $r = 10$ m.

3.3.2   Results and Discussions

We simulated the six different BSP schemes in the above and evaluated their relative performance in terms of network lifetime and amount of data delivered during the network lifetime. First, we illustrate the number of packets delivered to the base station(s) in a round as a function of time (measured in number of rounds) for a given realization of the distribution of the sensor nodes. Figures 3.3 and 3.4 show this behaviour of number of packets delivered in a round over time; Fig. 3.3 shows the traces for schemes 1), 2) and 6), and Fig. 3.4 shows the traces for the proposed schemes 3), 4) and 5).

From Fig. 3.3, it can be seen that the network life ends at the 27th round itself in the case of single static base station (scheme 1), whereas with three static base stations (scheme 2) the network life extends to 97 rounds. This is expected since, as we pointed out earlier, in the one base station case, the average hop length required to deliver a packet to the base station (and hence the energy spent) is more compared to the three static base stations case. The network life is further extended to 167 rounds when mobile base stations are deployed at the locations solved by the ILP at the beginning of each
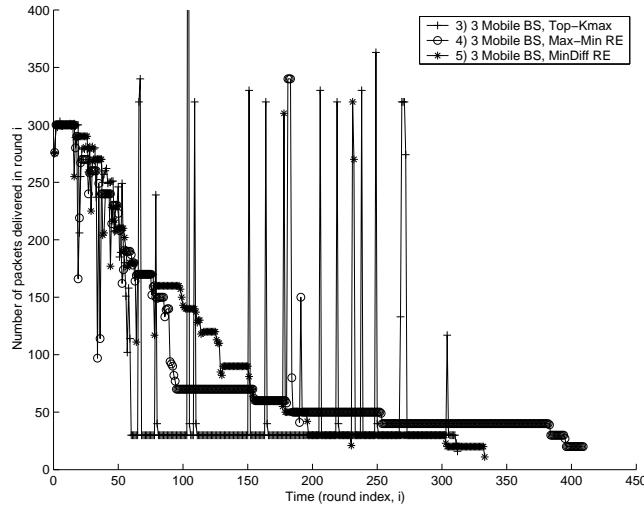
Figure 3.4: Traces of number of packets delivered per round as a function of time for the proposed schemes 3), 4), and 5). MCF routing. Initial energy at each node, $E_{battery} = 0.05$ J. One packet $= 200$ bits. Range of each node, $r = 10$ m.

round (scheme 6). Also, it is seen that the number of packets delivered in a round decreases as the round index (i.e., time) increases. This is because when nodes expire (indicated by the round indices where sharp fall and immediate rise of number of packets delivered are seen), the total rate of generation of new packets in the network reduces which reduces the maximum number of packets delivered in a round. The sharp fall in the number of packets delivered in a round is attributed to a node expiring in the middle of a round (typically, this node could be the first hop node to a base station), the expiry of which stops packet delivery to the base station till the end of that round. The number of packets delivered rises sharply in the very next round since a new set of base station locations are found (in case of scheme 6) and the routing gets updated (in all the schemes 1,2, and 6) at the beginning of the very next round. It can be further noted that the area under the trace for a given BSP scheme gives the total number of packets delivered in the entire network lifetime in that scheme.

From Fig. 3.4, we observe that the network lifetime achieved by the proposed BSP algorithms are significantly higher; 312 rounds for Top-K_{max} algorithm (scheme 3), 365 rounds for Max-Min-RE algorithm (scheme 4), and 380 rounds for Min-Diff-RE algorithm
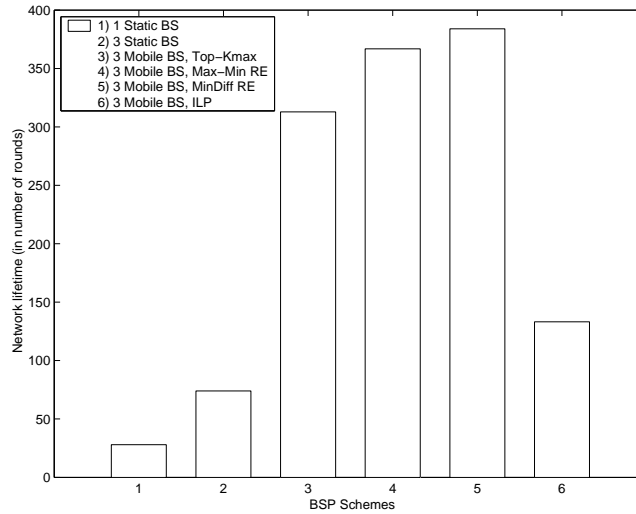
Figure 3.5: Network lifetime in number of rounds for different BSP algorithms. MCF routing. Initial energy at each node, $E_{battery} = 0.05$ J. One packet = 200 bits. Range of each node, $r = 10$ m.

(scheme 5). The high variability of the number of packets delivered in a round for the Top-K_{max} algorithm (mainly after round 60 in Fig. 3.4) can be attributed to the following: many of the 'close' neighbours of the feasible sites expire before the 60th round, during which time other nodes buffer many transit packets, and, when these nodes get selected as the first-hop neighbour node in the next rounds, all these buffered packets get delivered (which in turn consumes large amount of energy that can make the node expire) resulting in the sharp peaks. The variation of the number of packets delivered per round is more smooth in the Min-Max-RE and MinDiff-RE algorithms. The long tail in the traces of Max-Min-RE and MinDiff-RE algorithms indicate the possibility of just a few (typically one or two) nodes remaining alive in the network within the connectivity range of the feasible site(s); these nodes need much less energy since they need to transmit mainly their own packets (and very few transit packets from other nodes) because of which they survive longer keeping the network alive.

Next, in Fig. 3.5, we illustrate the average network lifetime performance of the various BSP algorithms. The network lifetimes for various BSP schemes shown in Fig. 3.5 are the simulated lifetimes averaged over 100 independent realizations of the distribution of the
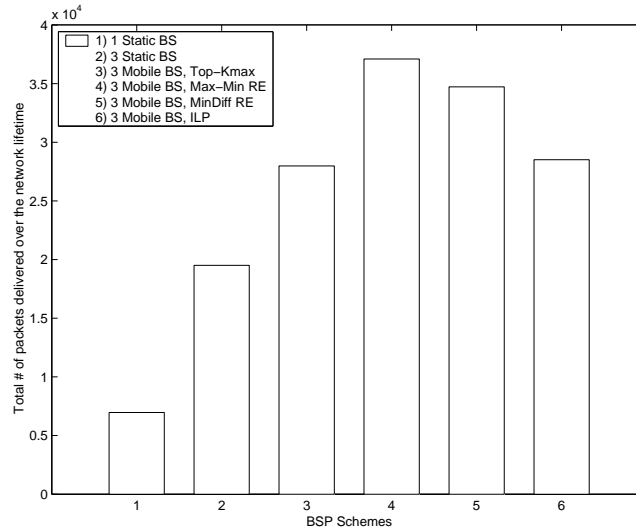
Figure 3.6: Amount of packets delivered during network lifetime for different BSP algorithms. MCF routing. Initial energy at each node, $E_{battery} = 0.05$ J. One packet = 200 bits. Range of each node, $r = 10$ m.

locations of the sensor nodes. For the same simulation runs, Fig. 3.6 shows the amount of data delivered during the network lifetime for the different BSP algorithms. The 95% confidence interval for the simulation results plotted in Figs. 3.5 and 3.6 are tabulated in Table 3.1. From Figs. 3.5 and 3.6, it can be seen that the proposed BSP algorithms (schemes 3,4,5) perform better than the single base station scheme (scheme 1) and fixed three base station scheme (scheme 2). Among the proposed schemes, scheme 4 (Min-max-RE) and scheme 5 (MinDiff-RE) perform best, achieving highest network lifetimes (about 360 rounds) and largest amount of data delivered (about 3.5×10^4 packets). The proposed schemes 4 and 5 give longer lifetimes than scheme 6 since the proposed schemes effectively use the residual energy information of the various nodes.

The total available energy in the entire network is 1.5 J (i.e., 30 nodes each having an initial energy of 0.05 J). It would be of interest to know how this total available energy in the network has been utilized by the different BSP algorithms. Toward this end, in Fig. 3.7, we plot the total energy spent by different algorithms over the entire network lifetime (averaged over the 100 simulation runs as in Figs. 3.5 and 3.6). The
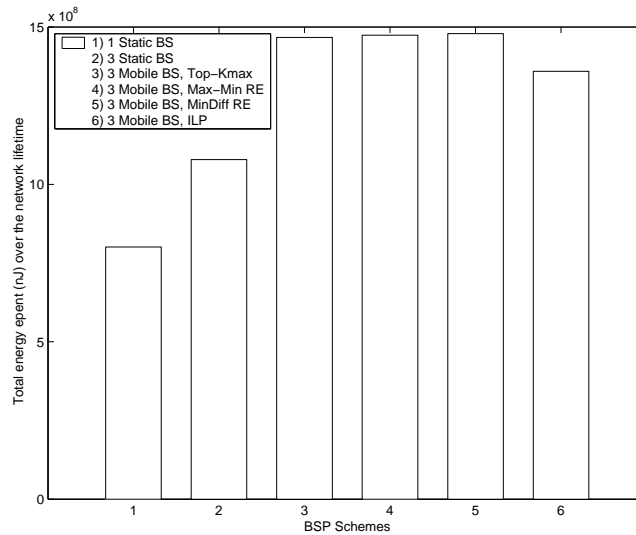
Figure 3.7: Total energy spent (in nJ) at the end of network life for different BSP algorithms. MCF routing. Initial energy at each node $E_{battery} = 0.05$ J. One packet = 200 bits. Range of each node, $r = 10$ m.

following three interesting observations can be made from Fig. 3.7. 1) All the three proposed algorithms (schemes 3,4,5) utilize almost all the available network energy of 1.5 J before the network life ends, whereas in the other algorithms significant amount of energy is left unused even at the end of the network life, 2) although Top-K_{max} algorithm utilizes almost all the network energy, it delivers much less number of packets compared to the Max-Min-RE and MinDiff-RE algorithms; however, Top-K_{max} algorithm has the advantage of lesser complexity, and 3) Max-Min-RE and MinDiff-RE algorithms perform well in terms of total energy spent, network lifetime, and amount of data delivered, but at a higher complexity compared to Top-K_{max} algorithm and lesser complexity compared to the ILP solution.

3.3.3 Energy Aware Routing

All the above performance results were obtained using MCF routing and they mainly quantified the performance benefit of using multiple base stations. It is noted that MCF routing is not energy aware and network lifetime can be further increased if energy aware

BSP Algorithm	NW lifetime in # rounds (95% confidence)	Data delivered in # packets (95% confidence)
1 BS	28 ± 0.009	$0.7 \times 10^4 \pm 0.34$
3 BS, static	74 ± 0.25	$1.9 \times 10^4 \pm 14.8$
3 BS, Top-K_{max}	312 ± 0.17	$2.8 \times 10^4 \pm 1.42$
3 BS, Max-Min-RE	365 ± 0.87	$3.7 \times 10^4 \pm 42.9$
3 BS, MinDiff-RE	380 ± 1.11	$3.5 \times 10^4 \pm 45.2$
3 BS, ILP	130 ± 0.45	$2.7 \times 10^4 \pm 76.5$

Table 3.1: Network lifetime and amount of data delivered for the various BSP schemes with MCF routing.

routing is used instead of MCF routing. We investigated the performance achieved using multiple base stations when an energy aware routing protocol that takes into account the residual energy at all nodes at the beginning of each round is employed. The energy aware routing protocol we used in this study is similar to the one given in [15], adapted to the multiple base stations case where the final destination for all the nodes is any one of the base stations. This energy aware routing protocol is run to obatin the routes at the beginning of each round. Let RE_i denote the residual energy at node i at the beginning of a round. The cost function to calculate the link cost between nodes i and j, $c_{i,j}$, is taken to be $c_{i,j} = e_{i,j}^{\alpha} RE_i^{-\beta}$, where α and β are non-negative numbers, $e_{i,j}$ is the energy required for node i to transmit one unit of information to its neighbouring node j. As in [15], we used $\alpha = 1$, $\beta = 50$ in our simulations. For each source node, the path to that base station towards which the path cost is minimum chosen.

Table 3.2 gives the simulated performance in terms of the network lifetime and amount of data delivered for the proposed MinDiff-RE algorithm as well as the ILP when energy aware routing is used. Similar performance results can be generated for the other BSP algorithms as well. Comparing the results in Tables 3.1 and 3.2, we can see that multiple base stations along with energy aware routing give increased network lifetimes and amount of data delivered.

BSP Algorithm	NW lifetime in # rounds (95% confidence)	Data delivered in # packets (95% confidence)
3 BS, Mindiff-RE	414 ± 1.9	$5.3 \times 10^4 \pm 557$
3 BS, ILP	218 ± 2.7	$4.5 \times 10^4 \pm 355$

Table 3.2: Network lifetime and amount of data delivered for the various BSP schemes with energy aware routing.

3.4   Conclusions

In this chapter, we proposed base stations placement algorithms to increase network lifetime and amount of data delivered during the lifetime in wireless sensor networks. We allowed multiple mobile base stations to be deployed along the periphery of the sensor network field and developed algorithms to dynamically choose the locations of these base stations so as to improve network lifetime. We proposed three energy efficient low-complexity algorithms to determine the locations of the base stations. We showed that the proposed base stations placement algorithms provide increased network lifetimes and amount of data delivered during the network lifetime compared to single base station scenario as well as multiple static base stations scenario. Energy aware routing is shown to result in additional gain in network lifetime.

Chapter 4

Cooperative Communication

Diversity techniques are well known for mitigating the effects of multipath fading and improving the reliability of communication in wireless channels [49],[50]. Spatial diversity techniques using multiple antennas at the receiver (receive diversity) are popular [51]. Recently, transmit diversity schemes have attracted much attention [52],[53]. Transmit diversity schemes require more than one antenna at the transmitter. However, many wireless devices (e.g., nodes in a sensor network) are limited by size or hardware complexity to one transmit antenna. Recently, a new class of methods called *cooperative communication* has been proposed that enables single-antenna mobiles in a multiuser environment to share their antennas and generate a virtual multiple-antenna transmitter that allows them to achieve transmit diversity [54],[55],[56].

4.1   Cooperative Diversity

Consider the three node network as shown in Fig. 1.2. A source node S wants to communicate with a destination node D. In a non-cooperative communication context, S would directly transmit to D. In a cooperative communication context, however, the relay node R can receive the transmission from S and forward it to D. This cooperative relaying essentially can provide a diversity path for D to demodulate data from S by observing the transmissions of both S as well as R. Diversity gains can be achieved

depending on the location of the relay node as well as the channel characteristics between S to R, S to D, and R to D. It is possible that the participation of the relay node can hurt the performance, particularly if the S to R link is of poor quality. Hence, use of relay node(s) for cooperation must be done judiciously. If multiple relays are used, it can essentially create multiple diversity paths for D.

4.2 Relay Protocols

The following relay protocols are common in a cooperative communication scenario.

4.2.1 Amplify-and-forward

Here, the relay acts as analog repeater by retransmitting an amplified version of its received signal from S. The noise floor is also amplified in the process. The destination node D will combine the information received from the source node S as well as the relay nodes R, and make a final decision on the transmitted symbol/packet.

4.2.2 Decode-and-Forward

Here, the relay attempts to decode, regenerate and retransmit a copy of the original signal received from S. With this Decode-and-Forward protocol scheme, it is possible that the relay forwards an erroneous estimate of the sender's symbol/packet, in which case cooperation can be detrimental to the eventual detection of the symbol/packet at the destination node D.

4.2.3 Decode-and-Re-encode

Decode and re-encode is a method that integrates cooperation into channel coding. The relay attempts to decode and construct codewords that are different from the received codewords, thereby providing incremental redundancy to a receiver that assesses the original and the re-encoded signals. Here again, there is the problem of error propagation.

4.3   Cooperative Diversity in Multihop Networks

Several studies have been reported on the simple single relay (two-hop) network model shown in Fig. 1.2 [49]-[57]. Performance results of cooperative diversity in terms of outage probability [56], information theoretic metrics [54], and symbol error probability expressions [55],[63],[64], and diversity gains on Rayleigh fading channels have been reported in the literature. The broadcast nature of the wireless the medium can be exploited to achieve cooperative diversity benefits in a *multihop wireless network* [65],[57]. Such a scenario where the intermediate nodes can act as cooperating relays is shown is illustrated in Fig. 4.1. In Fig. 4.1 (a), the traffic from source node A is routed to the destination node D via the intermediate nodes B and C without cooperation (i.e., conventional multihop routing without cooperation). Figure 4.1 (b), on the other hand, illustrates the same scenario as in Fig. 4.1 (a), but with cooperation. Here, the intermediate node E acts as a cooperating relay for the transmission from A to B. Likewise, node F acts as a cooperating relay for the transmission from C to D.

Cooperative Diversity to Enhance Network Lifetime

The potential benefit of cooperation shown in Fig. 4.1 (b) in a network-wide context can be highlighted as follows. At the link level, because of the potential diversity gains in the reception at nodes B and D due to cooperation, the transmit powers required to achieve a desired bit error performance on these links gets reduced. At the network level, these power savings at the nodes can increase the network lifetime, which is crucial in wireless sensor networks. Our interest in this chapter, accordingly, is to investigate the benefit of cooperation in enhancing the lifetime of wireless sensor networks. We consider a sensor network with a single base station as the data sink. Also, we consider the amplify-and-forward protocol in our study in this chapter. Other relaying protocols including decode-and-forward protocol and multiple base stations scenario can be considered as future studies. Closely following the analysis in Chapter 2, we present upper bounds on the network lifetime without and with cooperation using amplify-and-forward protocol. We also present simulation results that illustrate the lifetime enhancement due
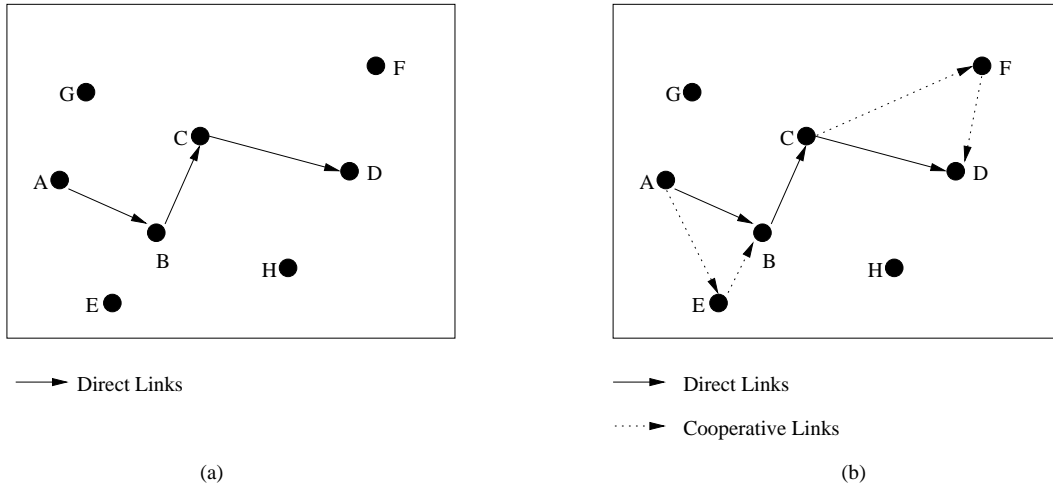
Figure 4.1: Multihop routing without and with cooperation.

to cooperation.

4.4   Bound on Lifetime without/with Cooperation

We are interested in obtaining upper bounds on the network lifetime without and with cooperative diversity. We consider a wireless sensor network scenario with one base station and N sensor nodes, each sensor node having a initial battery energy of E_{battery} joules as shown in Fig. 2.3. Consider all the links in the network to be independent Rayleigh faded. Consider BPSK modulation on all links. Let the desired bit error probability (BEP) on all links to be $P_e^{(\text{desired})}$.

Transmission without Cooperation

For the case of a Rayleigh faded link without cooperation, the BEP expression for BPSK is given by [49]

$$p_e = \frac{1}{2}\left(1 - \sqrt{\frac{\gamma}{1+\gamma}}\right). \tag{4.1}$$

where γ is the average signal-to-noise ratio (SNR) on the link. For high SNRs, (4.1) can be approximated to be

$$p_e \approx \frac{1}{4\gamma}. \tag{4.2}$$

The minimum transmit power required to establish the desired the BEP is then given by

$$P_T^{(\text{min})} = \frac{N_0}{4\Omega^2 p_e^{(\text{desired})}} \frac{d^\eta}{C}, \tag{4.3}$$

where d is the distance between the transmitter and receiver, η, is the path loss exponent, Ω^2 is the average fade power, N_0 is the additive white Gaussian noise variance, and C is a antenna gain and propagation factor given by [49]

$$C = \frac{G_t G_r \lambda^2}{(4\pi d)^2}, \tag{4.4}$$

where λ is the carrier wavelength, and G_t and G_r are the gains of the transmitting antenna and receive antennas, respectively. Here, we assume $G_t = G_r = 1$ and a carrier frequency of 900 MHz (i.e., $\lambda = 1/3$ m).

Using the minimum transmit power in (4.3), an approach similar to the one used in Chapter 2 can be adopted here to obtain upper bounds on network lifetime for the case of transmission between nodes without cooperation as follows. The energy spent by the receive electronics in an intermediate node to receive one bit, α_1, here is the same as in (2.2) in Sec. 2. However, the energy spent by the transmit electronics in sending on bit, α_2, in this case is given by

$$\alpha_2 = \frac{P_T^{(\text{min})}}{rd^\eta}, \tag{4.5}$$

where r is the transmission rate is bits/sec and P_T^{min} is given by (4.3). Using the α_1 and α_2 parameters from the above, the upper bound on the lifetime for this system model can be computed from (2.13).

Transmission with Cooperation

In this case, a cooperating relay node R participates and provides a diversity path for the transmission between a node A to node B. We consider the amplify-and-forward protocol at the cooperating node R. The BEP expression for BPSK on Rayleigh fading with cooperation using amplify-and-forward protocol is given by [63]

$$p_{e,AF} = \frac{3}{16}\left(\frac{1}{\gamma_{12}} + \frac{1}{\gamma_{23}}\right)\frac{1}{\gamma_{13}}, \tag{4.6}$$

where γ_{12}, γ_{23} and γ_{13} are the average SNRs on the links from A to R, R to B, and A to B, respectively, which are given by

$$\gamma_{12} = \frac{P_T\, C\, \Omega_{12}^2\, d_{12}^{-\eta}}{N_0}, \tag{4.7}$$

$$\gamma_{23} = \frac{P_T\, C\, \Omega_{23}^2\, d_{23}^{-\eta}}{N_0}, \tag{4.8}$$

and

$$\gamma_{13} = \frac{P_T\, C\, \Omega_{13}^2\, d_{13}^{-\eta}}{N_0}, \tag{4.9}$$

where C is given by (4.4), d_{12}, d_{23}, and d_{13} are the distances between nodes A to R, R to B, and A to R, respectively. Similarly, Ω_{12}, Ω_{23}, and Ω_{13} are the average fade powers on the links between nodes A to R, R to B, and A to R, respectively. Substituting (4.7), (4.8), and (4.9) in (4.6), and differentiating (4.6) w.r.t the location of R between A and B, we can see that the optimum location of R is the midpoint between the locations of A and B. From this observation, and from Eqns. (4.7), (4.8), (4.9), and (4.6), the minimum transmit power required to achieve a desired BEP at node B, can hence α_2, the total energy spent by the transmit electronics in sending one bit in this scenario with cooperation, $\alpha_{2,coop}$ can be obtained. Also, the total energy spent by the receive electronics for receiving a bit in the case of cooperation, $\alpha_{1,coop}$, is given by $2\alpha_{12} + 3\alpha_{11}$

Scenario	NW lifetime Upper Bound
No cooperation	57
Cooperation	75

Table 4.1: Upper bounds on network lifetime and without and with cooperation.

since one extra receive operation is required at the cooperating node compared to the case of no cooperation. Using the above $\alpha_{1,coop}$, and $\alpha_{2,coop}$, the upper bound on network lifetime for the case of cooperation can be computed from (2.13).

We computed the upper bounds for the cases of without and with cooperation in the above, and the results are shown in Table 4.1. From Table 4.2, we can see that cooperation shows larger network life compared to no cooperation. In addition to the comparison using analytical network lifetime bounds, we also carried out simulations to compare lifetime achieved without and with cooperation in the following section.

4.5   Simulation Results

We consider the following simulation model. A network region of dimension 1000 m $\times$ 1000 m with N sensor nodes uniformly distributed in network area is considered. The base station is located at the midpoint of one of the sides, i.e., at (0, 500). As in the previous chapters, here also we used the SMAC protocol in [27] for contention-free media access. Minimum hop routing is employed to select the routes from the nodes to the base station. All the links in the network are assumed to be independent Rayleigh faded. A cooperation node between a pair of nodes is chosen to be that node with the maximum residual energy among the nodes which are in the range of both the nodes. If there are no nodes in the common range of both the nodes, then a direct transmission without cooperation takes place. A packet is said to be received correctly at a node if the received SNR (combined SNR due to the source and cooperating node's transmissions if there is cooperation in the link) is greater than a desired SNR threshold, which depends on the

Scenario	NW lifetime in # rounds (95% confidence)	Data delivered in # packets (95% confidence)
No cooperation	55 ± 0.28	$2.7 \times 10^4 \pm 138$
Cooperation	58 ± 0.18	$2.85 \times 10^4 \pm 88$

Table 4.2: Network lifetime and amount of data delivered without and with cooperation.

modulation and receiver type used. Packets which do not satisfy this threshold condition are assumed to be dropped.

The network life time (in number of rounds) and amount of data delivered (in number of packets) during the network lifetime without and with cooperation obtained from the simulations are given in Table 4.2. It is observed that the network lifetime and amount of data delivered are more with cooperation than without cooperation. This illustrates the potential benefit of network lifetime enhancement using cooperative diversity. We further point out that cooperation can potentially hurt performance if the cooperating nodes are not properly chosen. For example, if the link quality between the source and cooperating nodes is poor then cooperation can degrade performance. In such cases, a threshold based cooperating node selection can be adopted. Optimum selection of cooperating nodes and optimizing system parameters including cooperating node selection threshold, number of cooperating nodes for network lifetime improvement can be investigated as further research. Cooperative diversity in the presence of multiple base stations can be also investigated as further extension to this work.

Chapter 5

Conclusions

In this thesis, we investigated multiple base stations approach to enhance lifetime in wireless sensor networks. First, we addressed the fundamental question concerning the limits on the network lifetime in sensor networks with multiple base stations. We derived upper bounds on the network lifetime when multiple base stations are deployed along the boundary of the sensing field. We also obtained optimum locations of the base stations that maximize these network lifetime bounds. For a scenario with single base station and a rectangular region of observation, we obtained closed-form expressions for the network lifetime bound and the optimum base station location. For the case of two base stations, we jointly optimized the base station locations by maximizing the lifetime bound using a genetic algorithm based optimization. Since joint optimization for more number of base stations is complex, for the case of three base stations, we optimized the third base station location using the previously obtained optimum locations of the first two base stations. We also provided simulation results that validated the network lifetime bounds and the optimal choice of the locations of the base stations.

Next, we considered algorithms for placement of multiple mobile base stations in wireless sensor networks. We allowed multiple mobile base stations to be deployed along the periphery of the sensor network field and developed algorithms to dynamically choose the locations of these base stations so as to improve network lifetime. We proposed three energy efficient low-complexity algorithms to determine the locations of the base

stations. We showed that the proposed base stations placement algorithms provide increased network lifetimes and amount of data delivered during the network lifetime compared to single base station scenario as well as multiple static base stations scenario.

Finally, we briefly investigated the benefit of employing cooperative diversity in enhancing the lifetime of wireless sensor networks. By considering a single base station scenario and using an amplify-and-forward relay protocol, we illustrated the benefit of employing cooperation compared to no cooperation through bounds and simulations.

As further extension to this work optimum selection of cooperating nodes and optimizing system parameters including cooperating node selection threshold, number of cooperating nodes for network lifetime improvement can be considered. Also Cooperative diversity in the presence of multiple base stations can be also investigated as further extension to this work.

Appendix A

Derivation of Lifetime Upper Bound for Two Base Stations Case

In this Appendix, we derive the lifetime upper bounds for two base stations case with same side orientation (SSO) and opposite side orientation (OSO).

Same Side Orientation

First, consider the case of same side orientation (SSO) shown in Fig. A.1. For the placement of B_1 and B_2 on the W side, the partitioning axis $Y_a Y_b$ is represented by the straight line, where $Y_a = Y_b = (z_1 + z_2)/2$. For this SSO case, the analysis of ASO case applies with the limits $(x_1, x_2), (x_3, x_4), \cdots, (x_7, x_8)$ and $(y_1, y_2), (y_3, y_4), \cdots, (y_7, y_8)$ in the integrals in Eqns. (2.24) and (2.25) to be $(x_3, x_4) = (y_3, y_4) = (x_7, x_8) = (y_7, y_8) = (0, 0)$, $(x_1, x_2) = (0, L)$, $(y_1, y_2) = (-z_1, (z_2 - z_1)/2)$, $(x_5, x_6) = (0, L)$, and $(y_5, y_6) = (-(z_2 - z_1)/2, W - z_2)$. Similarly, for the case of placement of B_1 and B_2 on the L side, the partitioning axis is the line $X_a X_b$ where $X_a = X_b = (z_1 + z_2)/2$ in Fig. A.1(b). For this case, the limits in the integrals in Eqns. (2.24) and (2.25) are given by $(x_3, x_4) = (y_3, y_4) = (x_7, x_8) = (y_7, y_8) = (0, 0)$, $(x_1, x_2) = (-z_1, (z_2 - z_1)/2)$, $(y_1, y_2) = (0, W)$ $(x_5, x_6) = (-(z_2 - z_1)/2, L - z_2))$, and $(y_5, y_6) = (0, W)$. Using the above, the optimum locations of base stations for SSO $(z_{1,\text{opt}}, z_{2,\text{opt}})_{\text{sso}}$ that maximizes the SSO lifetime upper bound $\mathcal{T}_{2\text{-BS,sso}}^{(z_1, z_2)}$ can be computed.

a) partition along $Y_a Y_b$ axis

B_1 and B_2 are located on W side

a) partition along $X_a X_b$ axis

B 1 and B 2 are located on L side
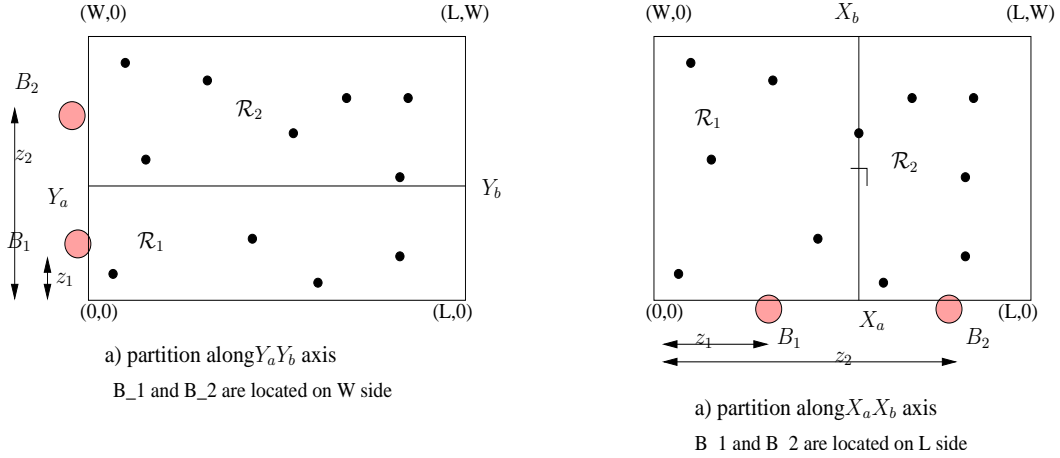
Figure A.1: Same side orientation (SSO) of two base stations.

Opposite Side Orientation

Next, consider the case of opposite side orientation (OSO).

B_1 and B_2 on L Side:

Consider the OSO case with B_1 and B_2 located on the L side as shown in Fig. A.2. For a given z_1 and z_2, the partition axis will belong to any of the following possible axis types i) $Y_a Y_b$, $X_a Y_b$, $Y_a X_b$, and $Y_a Y_b$ when $z_1 \geq z_2$, and ii) $Y_a Y_b$, $X_a Y_b$, $Y_a X_b$, and $Y_a Y_b$ when $z_1 \leq z_2$, as shown in Figs. A.2(a) to (h). Again, The partition axis can be represented by the straight line

$$Y = mX + c, \tag{A.1}$$

where $m = \frac{W}{z_2 - z_1}$ and $c = \frac{W^2 - (z_1^2 - z_1^2)}{2W}$. Then, from (A.1) we have

$$X_a = X|_{Y=0} \implies X_a = -\frac{c}{m} = \frac{W^2 - (z_1^2 - z_1^2)}{2W}, \tag{A.2}$$

$$X_b = X|_{Y=W} \implies X_b = \frac{W - c}{m} = \frac{W}{z_1 - z_2} - \frac{W^2 - (z_1^2 - z_1^2)}{2(z_1 - z_2)}, \tag{A.3}$$

$$Y_a = Y|_{X=0} \implies Y_a = c = \frac{W^2 - (z_1^2 - z_1^2)}{2W}, \tag{A.4}$$

Limits	For Y_aY_b axis Fig.A.2(a)	For X_aY_b axis Fig.A.2(b)	For Y_aX_b axis Fig.A.2(c)	For X_aX_b axis Fig.A.2(d)
(x_1, x_2)	$(-z_2, L - z_2)$	$(-z_2, X_a - z_2)$	$(-z_2, X_b - z_2)$	$(-z_2, X_a - z_2)$
(y_1, y_2)	$(0, -Y_{z_2})$	$(0, W)$	$(0, -Y_{z_2})$	$(0, W)$
(x_3, x_4)	$(0, 0)$	$(X_a - z_2, L - z_2)$	$(0, 0)$	$(X_a - z_2, X_b - z_2)$
(y_3, y_4)	$(0, 0)$	$(0, Y_{z_2})$	$(0, 0)$	$(0, -Y_{z_2})$
(x_5, x_6)	$(-z_1, L - z1)$	$(X_a - z_1, L - z_1)$	$(-z_1, X_b - z_1)$	$(X_a - z_1, X_b - z_1)$
(y_5, y_6)	$(0, Y_{z_1})$	$(0, Y_{z_1})$	$(0, Y_{z_1})$	$(0, Y_{z_1})$
(x_7, x_8)	$(0, 0)$	$(0, 0)$	$(X_b - z_1, L - z_1)$	$(X_b - z_1, L - z_1)$
(y_7, y_8)	$(0, 0)$	$(0, 0)$	$(0, W)$	$(0, W)$

Table A.1: Limits $y_1, y_2, \cdots, y_8$ and $x_1, x_2, \cdots, x_8$ in (2.24) and (2.25) for two base station OSO for various partition axis types in Figs. A.2 (a), (b), (c) and (d).

$$Y_b = Y|_{X=L} \implies Y_b = mL + c = \frac{L(z_1 - z_2)}{W} + \frac{W^2 - (z_1^2 - z_1^2)}{2W}. \qquad (A.5)$$

For a given z_1 and z_2, $z_1 \geq z_2$, the partition axis type is

i) Y_aY_b if $Y_a \geq 0$ and $Y_b \leq W$ (Fig. A.2(a)), ii) X_aY_b if $X_a \geq 0$ and $Y_b \leq W$ (Fig. A.2(b)),

iii) Y_aX_b if $Y_a \geq 0$ and $X_b \leq L$ (Fig. A.2(c)), iv) Y_aY_b if $Y_a \geq 0$ and $Y_b \leq W$ (Fig. A.2(d)),

and when $z_1 \leq z_2$, the partition axis type is

v) Y_aY_b if $Y_b \geq 0$, and $Y_a \leq W$ (Fig. A.2(e)), vi) X_bY_b if $X_a \geq 0$ and $X_b \geq 0$ (Fig. A.2(f)),

vii) Y_aX_a if $Y_a \leq W$ and $X_a \leq L$ (Fig. A.2(g)), viii) X_aX_b if $X_a \leq L$ and $X_b \geq W$ (Fig. A.2(h)).

Defining $Y_{z_1} = Y|_{X=x+z_1}$ and $Y_{z_2} = Y|_{X=x+z_1} - W$ in (A.1), the limits $y_1, y_2, \cdots, y_8$ and $x_1, x_2, \cdots, x_8$ in the integrals in (2.24) and (2.25) for the various partition axis types in Figs. A.2 (a), (b), (c), and (d) are given in Table A.1. Similarly, the limits for the partition axis types in Figs. A.2 (e), (f), (g), and (h) are given in Table A.2.

B_1 and B_2 on W Side:

Next, consider OSO with B_1 and B_2 located on the W side as shown in Fig. A.3. For this case, the m and c in (A.1) are given by where $m = \frac{L}{z_1 - z_2}$ and $c = \frac{(z_1^2 - z_1^2)^2 - L^2}{2(z_1 - z_2)}$, and X_a and X_b are given ny
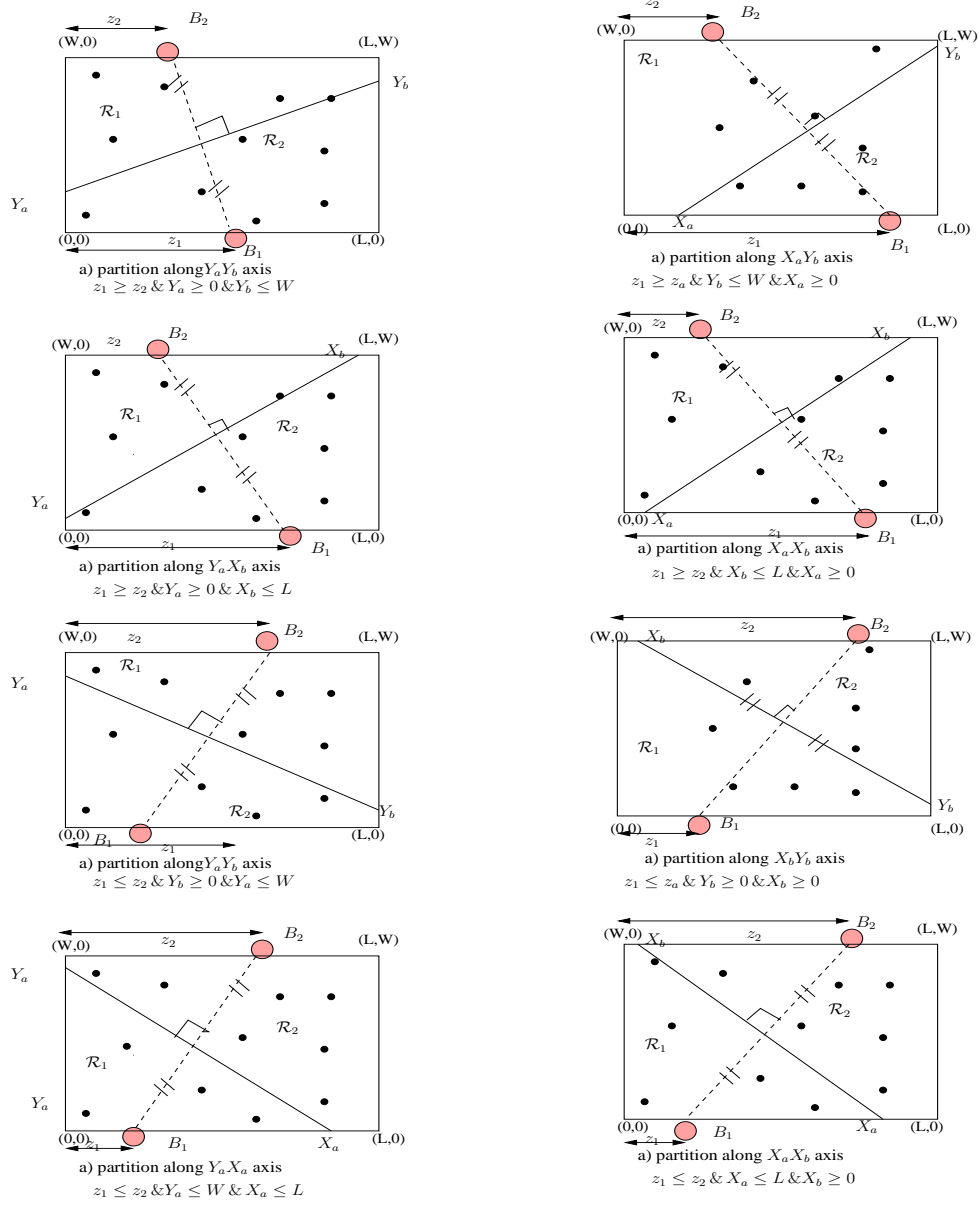
Figure A.2: Different partitioning axis types for opposite side orientation (OSO) of two base stations with B_1 and B_2 on L side.

Limits	For $Y_a Y_b$ axis Fig.A.2(e)	For $X_b Y_b$ axis Fig.A.2(f)	For $Y_a X_b$ axis Fig.A.2(g)	For $X_a X_b$ axis Fig.A.2(h)
(x_1, x_2)	$(-z_2, L-z_2)$	$(X_b-z_2, L-z_2)$	$(-z_2, X_a-z_2)$	(X_b-z_2, X_a-z_2)
(y_1, y_2)	$(0, -Y_{z_2})$	$(0, -Y_{z_2})$	$(0, -Y_{z_2})$	$(0, Y_{z_2})$
(x_3, x_4)	$(0, 0)$	$(0, 0)$	$(X_a-z_2, L-z_2)$	$(X_a-z_2, L-z_2)$
(y_3, y_4)	$(0, 0)$	$(0, 0)$	$(0, W)$	$(0, W)$
(x_5, x_6)	$(-z_1, L-z1)$	$(-z_1, X_b-z_1)$	$(-z_1, X_b-z_1)$	$(-z_1, X_b-z_1)$
(y_5, y_6)	$(0, Y_{z_1})$	$(0, W)$	$(0, Y_{z_1})$	$(0, L)$
(x_7, x_8)	$(0, 0)$	$(X_b-z_1, L-z_1)$	$(0, 0)$	(X_b-z_1, X_a-z_1)
(y_7, y_8)	$(0, 0)$	$(0, Y_{z_1})$	$(0, 0)$	$(0, Y_{z_1})$

Table A.2: Limits $y_1, y_2, \cdots, y_8$ and $x_1, x_2, \cdots, x_8$ in (2.24) and (2.25) for OSO for various partition axis types in Figs. A.2 (e), (f), (g) and (h).

$$X_a = -\frac{(z_1^2 - z_1^2)^2 - L^2}{2L}, \tag{A.6}$$

$$X_b = \frac{L}{z_1 - z_2} - \frac{(z_1^2 - z_1^2)^2 - L^2}{2L}. \tag{A.7}$$

For a given z_1, z_2, the only partition axis type is $X_a X_b$ and $X_a \geq 0$ and $X_b \geq L$ is satisfied $\forall z_1, z_2$ (Fig. A.3). Defining $X_{z_1} = X|_{Y=y+z_1}$ and $X_{z_2} = Y|_{X=x+L, Y=y+z_2}$ in the $X_a X_b$ line, the limits $y_1, y_2, \cdots, y_4$ and $x_1, x_2, \cdots, x_4$ in the integrals in (2.24) and (2.25) for this case is given by $(x_1, x_2) = (0, X_{z_1})$,$(y_1, y_2) = (-z_1, W - z_1)$, $(x_3, x_4) = (0, X_{z_2})$, $(y_3, y_4) = (-z_2, W - z_2)$.

Using the above, the optimum locations of base stations for OSO $\left(z_{1,\mathrm{opt}}, z_{2,\mathrm{opt}}\right)_{\mathrm{oso}}$ that maximizes the OSO lifetime upper bound $\mathcal{T}_{2\text{-BS,oso}}^{(z_1, z_2)}$ can be computed.

(W,0) X_b (L,W)

$\mathcal{R}_1$

B_2

$\mathcal{R}_2$

B_1

z_2

z_1

(0,0) X_a (L,0)

a) partition along $X_a X_b$ axis

$X_a \geq 0 \, \& \, X_b \geq W \, \forall z_1, z_2$

B 1 and B 2 are located on W side
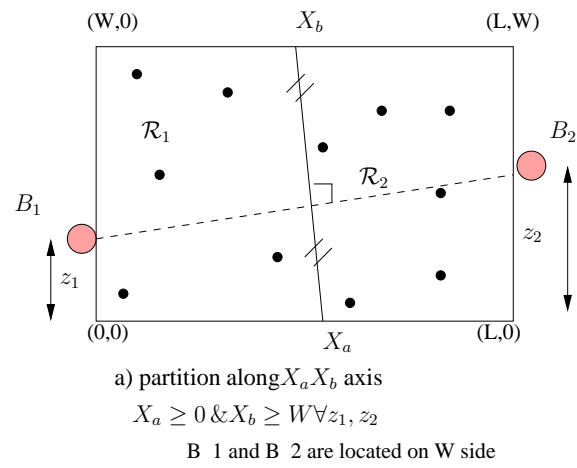
Figure A.3: Opposite side orientation of two base stations with B_1 and B_2 on W side.

Appendix B

Derivation of Lifetime Upper Bound for Three Base Stations Case

In this Appendix, we present the derivation of the network lifetime upper bound for the case of three base stations when $W \leq L/2$. Similar derivation can be done for the case of $L/2 < W \leq L$. As mentioned, we place base stations B_1 and B_2 in their individually optimal locations (as shown in Fig. 2.7), and determine the optimal location of the BS B_3 that maximize the upper bound on the network lifetime. To derive the network lifetime upper bound, we need to consider two cases of placing B_3; *a)* on the adjacent side (ASO as shown in Fig. 2.7(a)), and *b)* on the same side (SSO as shown in Fig. 2.7(b)).

Adjacent Side Orientation

From the solution of the two BS problem, we have the locations of B_1 and B_2 to be $(L/2, 0)$ and $(L/2, W)$, respectively, i.e., $z_1 = z_2 = L/2$ in Fig. 2.7. Since B_1 and B_2 are fixed, the axes along which the partition of regions $\mathcal{R}_1, \mathcal{R}_2$, and $\mathcal{R}_3$ occurs depends on the location of B_3 only. Since B_3 can be placed anywhere on the W side, we can see that $X_f \geq 0$ and $X_c \geq 0$ are always satisfied. Also, we can see that Y_b is always fixed. We have three partitioning axes $(X_c X_d), (X_e X_f), (Y_a Y_b)$ which divide the region $\mathcal{R}$ in three

Parameter	For $Y_a Y_b$ axis	For $X_c X_d$ axis	For $X_e X_f$ axis
m	$-\dfrac{(z_2 - z_1)}{W}$	$\dfrac{z_1}{z_3}$	$\dfrac{z_2}{z_3 - W}$
c	$\dfrac{W^2 - (z_1{}^2 - z_2{}^2)}{2W}$,	$\dfrac{z_3{}^2 - k_1{}^2}{2z_3}$	$\dfrac{z_3{}^2 - W^2 - z_3{}^2}{2(z_3 - W^2)}$

Table B.1: Parameters m and c in Eqn. (B.1) for different partition axes in the three base station problem for the case of ASO.

parts as shown in Fig. 2.7(a). Each partition axis can be represented by a straight line

$$Y = mX + c, \tag{B.1}$$

where m, c for various axes are given in Table B.1. Then, from (B.1), we have

$$Y_a = Y|_{X=0} \implies Y_a = c = \frac{W^2 - (z_1^2 - z_2^2)}{2W}, \tag{B.2}$$

$$Y_b = Y|_{X=L} \implies Y_b = mL + c = \frac{L(z_1 - z_2)}{W} + \frac{W^2 - (z_1^2 - z_2^2)}{2W}. \tag{B.3}$$

Also,

$$X_c = X|_{Y=0} \implies X_c = -\frac{c}{m} = -\frac{z_3^2 - z_1^2}{2z_1}, \tag{B.4}$$

$$X_d = X|_{Y=W} \implies X_d = \frac{W - c}{m} = \frac{W z_3}{z_1} - \frac{z_3^2 - z_1^2}{2z_1}, \tag{B.5}$$

and

$$X_e = X|_{Y=0} \implies X_e = -\frac{c}{m} = -\frac{z_3^2 - W^2 - z_2^2}{2(z_3 - W)}, \tag{B.6}$$

$$X_f = X|_{Y=W} \implies X_f = \frac{W - c}{m} = \frac{W(z_3 - W)}{z_2} - \frac{z_3^2 - W^2 - z_2^2}{2z_2}. \tag{B.7}$$

Now, the energy dissipation in the entire network with base station locations z_1, z_2, and z_3 for the ASO case is given by

$$P_{\text{NW,aso}}^{(z_1,z_2,z_3)} = N \left(\int \int_{\mathcal{R}_1} P_{\text{nw}}(x,y) \frac{1}{WL} \, dx \, dy + \int \int_{\mathcal{R}_2} P_{\text{nw}}(x,y) \frac{1}{WL} \, dx \, dy \right.$$
$$\left. + \int \int_{\mathcal{R}_3} P_{\text{nw}}(x,y) \frac{1}{WL} \, dx \, dy \right). \tag{B.8}$$

By the minimum energy relay argument, we have $P_{\text{nw}}(x,y) \geq P_{\text{link}}\left(\sqrt{x^2+y^2}\right)$, where $P_{\text{link}}(D)$ is given by (2.7). Hence,

$$P_{\text{NW,aso}}^{(z_1,z_2,z_3)} \geq \frac{N}{WL} \left(\int \int_{\mathcal{R}_1} P_{\text{link}}\left(\sqrt{x^2+y^2}\right) dx \, dy + \int \int_{\mathcal{R}_2} P_{\text{link}}\left(\sqrt{x^2+y^2}\right) dx \, dy \right.$$
$$\left. + \int \int_{\mathcal{R}_3} P_{\text{link}}\left(\sqrt{x^2+y^2}\right) dx \, dy \right)$$
$$\geq \frac{r\alpha_1}{d_{char}} \frac{\eta}{\eta-1} \frac{N}{WL} \left(\int \int_{\mathcal{R}_1} \sqrt{x^2+y^2} \, dx \, dy + \int \int_{\mathcal{R}_2} \sqrt{x^2+y^2} \, dx \, dy + \int \int_{\mathcal{R}_3} \sqrt{x^2+y^2} \, dx \, dy \right)$$
$$\geq \frac{r\alpha_1}{d_{char}} \frac{\eta}{\eta-1} \frac{N}{WL} \left[d_{\text{3-BS,aso}}^{\mathcal{R}_1}(z_1,z_2,z_3) + d_{\text{3-BS,aso}}^{\mathcal{R}_2}(z_1,z_2,z_3) + d_{\text{3-BS,aso}}^{\mathcal{R}_3}(z_1,z_2,z_3) \right], \tag{B.9}$$

where $d_{\text{3-BS,aso}}^{\mathcal{R}_1}(z_1,z_2,z_3)$, $d_{\text{3-BS,aso}}^{\mathcal{R}_2}(z_1,z_2,z_3)$ and $d_{\text{3-BS,aso}}^{\mathcal{R}_3}(z_1,z_2,z_3)$ are of the form

$$d_{\text{3-BS,aso}}^{\mathcal{R}_1}(z_1,z_2,z_3) = \int_{y_1}^{y_2} \int_{x_1}^{x_2} \sqrt{x^2+y^2} \, dx \, dy + \int_{y_3}^{y_4} \int_{x_3}^{x_4} \sqrt{x^2+y^2} \, dx \, dy, \tag{B.10}$$

$$d_{\text{3-BS,aso}}^{\mathcal{R}_2}(z_1,z_2,z_3) = \int_{x_5}^{x_6} \int_{y_5}^{y_6} \sqrt{x^2+y^2} \, dy \, dx + \int_{x_7}^{x_8} \int_{y_7}^{y_8} \sqrt{x^2+y^2} \, dy \, dx, \tag{B.11}$$

and

$$d_{\text{3-BS,aso}}^{\mathcal{R}_3}(z_1,z_2,z_3) = \int_{x_9}^{x_{10}} \int_{y_9}^{y_{10}} \sqrt{x^2+y^2} \, dy \, dx + \int_{x_{11}}^{x_{12}} \int_{y_{11}}^{y_{12}} \sqrt{x^2+y^2} \, dy \, dx. \tag{B.12}$$

Now, denoting (X_I, Y_I) to be the coordinates of the point of intersection of the three axes Y_aY_b, X_cX_d and X_eX_f, we have

$$X_I = \frac{c_2 - c_1}{m_1 - m_2}, \tag{B.13}$$

Limits		Values	
(x_1, x_2)	(y_1, y_2)	$(0, X_{l_2 z_3})$	$(-z_3, Y_I - z_3)$
(x_3, x_4)	(y_3, y_4)	$(0, X_{l_3 z_3})$	$(Y_I - z_3, W - z_3)$
(x_5, x_6)	(y_5, y_6)	$(X_f - z_2, X_I - z_2)$	$(0, -Y_{l_3 z_2})$
(x_7, x_8)	(y_7, y_8)	$(X_I - z_2, L - z_2)$	$(0, -Y_{l_1 z_2})$
(x_9, x_{10})	(y_9, y_{10})	$(X_c - z_1, X_I - z_1)$	$(0, Y_{l_2 z_1})$
(x_{11}, x_{12})	(x_{11}, x_{12})	$(X_I - z_1, L - z_1)$	$(0, Y_{l_1 z_1})$

Table B.2: Limits $y_1, y_2, \cdots, y_{12}$ and $x_1, x_2, \cdots, x_{12}$ in the integrals in Eqns. (B.10), (B.11), and (B.12) for the case of ASO.

and

$$Y_I = \frac{c_1 m_2 - c_2 m_1}{m_2 - m_1}, \tag{B.14}$$

where m_1, c_1 and m_2, c_2 are the m, c parameters for the $Y_a Y_b$ and $X_c X_d$ axes, respectively, as given in Table B.1. Also, define

$Y_{l_1 z_2} = Y|_{X = x + z_2} - W$ and $Y_{l_1 z_1} = Y|_{X = x + z_1}$ in the $Y_a Y_b$ line,

$X_{l_2 z_3} = X|_{Y = y + z_3}$ and $Y_{l_2 z_1} = Y|_{X = x + z_1}$ in the $X_c X_d$ line, and

$X_{l_3 z_3} = X|_{Y = y + z_3}$ and $Y_{l_3 z_2} = Y|_{X = x + z_2} - W$ in the $X_e X_f$ line.

Using the above definitions, we can write the limits of the integrals in Eqns. (B.10), (B.11) and (B.12) to be as given in Table B.2

Now, denoting $\mathcal{T}_{\text{3-BS,aso}}^{(z_1, z_2, z_3)}$ as the network lifetime with three base stations at locations z_1, z_2, z_3 for the ASO case, we have

$$P_{\text{NW,aso}}^{(z_1, z_2, z_3)} \mathcal{T}_{\text{3-BS,aso}}^{(z_1, z_2, z_3)} \leq NE_{\text{battery}}. \tag{B.15}$$

Hence, an upper bound on the network lifetime for a given (z_1, z_2, z_3) for the case of ASO can be obtained as

$$\mathcal{T}_{\text{3-BS,aso}}^{(z_1, z_2, z_3)} \leq \frac{NE_{\text{battery}}}{\frac{r\alpha_1}{d_{char}} \frac{\eta}{\eta - 1} \frac{N}{WL} \left(d_{\text{3-BS,aso}}^{\mathcal{R}_1}(z_1, z_2, z_3) + d_{\text{3-BS,aso}}^{\mathcal{R}_2}(z_1, z_2, z_3) + d_{\text{3-BS,aso}}^{\mathcal{R}_3}(z_1, z_2, z_3) \right)}. \tag{B.16}$$

The optimum base station locations for the ASO case that maximizes the above lifetime

Parameter	For $Y_a Y_b$ axis	For $X_c X_d$ axis	For $X_e Y_e$ axis
m	$-\frac{(z_2-z_1)}{W})$	∞	$-\frac{(z_2-z_3)}{W}$
c	$\frac{W^2+z_2{}^2-z_1{}^2}{2W}$	$-\infty$	$\frac{W^2+(z_2-z_3)(z_1+z_3)}{2(z_3-z^2)}$

Table B.3: Parameters m and c in Eqn. (B.1) for different partition axes in the three base station problem for the case of SSO.

bound is then given by

$$\left(z_{3,\text{opt}}\right)_{aso} = \underset{z_3 \in (0,W)}{\text{argmax}} \; \mathcal{T}_{3\text{-BS,aso}}^{(z_1,z_2,z_3)}. \tag{B.17}$$

Same Side Orientation

A similar approach can be adopted for the case of same side orientation (SSO) of the placement of B_3 as shown in Fig. 2.7(b). Here, the region $\mathcal{R}$ can be divided into $\mathcal{R}_1$, $\mathcal{R}_2$, and $\mathcal{R}_3$ using the partitioning axes $Y_a Y_b$, $X_c X_d$, and $X_e Y_e$, as shown in Fig. 2.7(b). The m and c parameters for these three axes are given in Table B.3. Also, the limits in the integrals of Eqns. (B.10), (B.11), and (B.12) for the case of SSO are given in Table B.4, where

$Y_{l_1 z_2} = Y|_{X=x+z_2} - W$ and $Y_{l_1 z_1} = Y|_{X=x+z_1}$ in the $Y_a Y_b$ line, and

$Y_{l_3 z_3} = Y|_{X=x+z_3}$ and $Y_{l_3 z_2} = Y|_{X=x+z_2} - W$ in the $X_e Y_e$ line.

Using the values in Tables B.3 and B.4, and following similar steps as in the case of ASO, the optimum location of B_3 for the case of SSO can be found as

$$\left(z_{3,\text{opt}}\right)_{sso} = \underset{z_3 \in (0,W)}{\text{argmax}} \; \mathcal{T}_{3\text{-BS,sso}}^{(z_1,z_2,z_3)}. \tag{B.18}$$

Limits		Values	
(x_1, x_2)	(y_1, y_2)	$(-z_3, X_c - z_3)$	$(0, Y_{l_3 z_3})$
(x_3, x_4)	(y_3, y_4)	$(0, 0)$	$(0, 0)$
(x_5, x_6)	(y_5, y_6)	$(-z_2, X_c - z_2)$	$(0, -Y_{l_3 z_2})$
(x_7, x_8)	(y_7, y_8)	$(X_c - z_2, L - z_2)$	$(0, -Y_{l_1 z_2})$
(x_9, x_{10})	(y_9, y_{10})	$(X_c - z_1, L - z_1)$	$(0, Y_{l_1 z_1})$
(x_{11}, x_{12})	(x_{11}, x_{12})	$(0, 0)$	$(0, 0)$

Table B.4: Limits $y_1, y_2, \cdots, y_{12}$ and $x_1, x_2, \cdots, x_{12}$ in Eqns. (B.10), (B.11), and (B.12) for the case of SSO.

Bibliography

[1] I. F. Akyildiz, W. Su, Y. Sankarasubramaniam, and E. Cayirci, "A survey on sensor networks," *IEEE Commun. Mag.,* pp. 102-114, August 2002.

[2] G. J. Pottie and W. J. Kaiser, "Wireless integrated network sensors," *Commun. of the ACM*, 43(5), pp. 51-58, 2000.

[3] A. Mainwaring, J. Polastre, R. Szewczyk, D. Culler, and J. Anderson, "Wireless sensor networks for habitat monitoring," *Proc. ACM Wireless Sensor Networks and Applications Workshop (WSNA'02),* 2002.

[4] P. Zuang *et al.,* "Energy-efficient computing for wildlife tracking: Design trade-offs and early experiences with zebranet," *Intl. Conf. on Architectural Support for Programming Languages and Operating Systems (ASPLOS)*, 2002.

[5] A. Beafour, M. Leopolad, and P. Bonnet, "Smart tag based data dissemination," *Proc. ACM Wireless Sensor Networks and Applications Workshop (WSNA'02),* 2002.

[6] I. F. Akyildiz and I. H. Kasimoglu, "Wireless sensor and actor networks: Research challenges," *Ad-hoc Networks Journal (Elsevier)*, vol. 2, pp. 351-367, October 2004.

[7] W. B. Heinzelman, A. P. Chandrakasan, and H. Balakrishnan, "Energy scalable algorithms and protocols for wireless sensor networks," *Proc. Intl. Conf. on Acoustics, Speech and Signal Processing (ICASSP'00),* Istanbul, Turkey, June 2000.

[8] W. B. Heinzelman, A. P. Chandrakasan, and H. Balakrishnan, "Energy efficient communication protocol for wireless sensor networks," *Proc. of the Hawaii Intl. Conf. System Sciences,* Hawaii, January 2000.

[9] W. B. Heinzelman, A. P. Chandrakasan, and H. Balakrishnan, "An application-specific protocol architecture for wireless microsensor networks," *IEEE Trans. Wireless Commun.,* vol. 1, no. 4, pp. 660-670, October 2002.

[10] W. Ye, J. Heidemann, and D. Estrin, "An energy efficient MAC protocol for wireless sensor networks," *Proc. MobiCom'01*, Rome, Italy, July 2001.

[11] V. Rodoplu and T. H. Meng, "Minimum energy mobile wireless networks," *Proc. IEEE ICC'98*, vol. 3, pp. 1633-1639, Atlanta, June 1998.

[12] A. Sankar and Z. Liu, "Maximum lifetime routing in wireless ad-hoc networks," *Proc. IEEE INFOCOM'04*, 2004.

[13] S. Singh, M. Woo, and C. S. Raghavendra, "Power-aware routing in mobile ad-hoc networks," *Proc. ACM/IEEE Intl. Conf. on Mobile Computing and Networking*, pp. 181-190, Dallas, October 1998.

[14] J.-H. Chang and L. Tassiulas, "Routing for maximum system lifetime in wireless ad-hoc networks," *Proc. 37th Ann. Allerton Conf. on Commun., Control, and Computing*, September 1999.

[15] J.-H. Chang and L. Tassiulas, "Energy conserving routing in wireless ad-hoc networks," *Proc. IEEE INFOCOM'00*, pp. 22-31, 2000.

[16] S. Lindsey and C. Raghavendra, "PEGASIS: Power-efficient gathering in sensor information systems, *Proc. IEEE ICC'2001*, 2001.

[17] S. Lindsey, C. S. Raghavendra, and K. Sivalingam, "Data gathering in sensor networks using the energy-delay metric," *Proc. IPDPD Workshop on Issues in Wireless Networks and Mobile Computing*, San Francisco, April 2001.

[18] A. Manjeshwar and D. P. Agrawal, "TEEN: A routing protocol for enhanced efficiency in wireless sensor networks," *Proc. 15th Intl. Parallel and Distributed Processing Symposium,* pp. 2009-2015, 2001.

[19] A. Manjeshwar and D. P. Agrawal, "APTEEN: A hybrid protocol for efficient routing and comprehensive information retrieval in wireless sensor networks," *Prof. of the 2nd Intl. Workshop on Parallel and Distributed Computing Issues in Wireless Networks and Mobile Networking,* Florida, April 2002.

[20] M. Younis, M. Youssef, and K. Arisha, "Energy aware routing in cluster based sensor networks," *Proc. Intl. Symp. on Modeling, Analysis and Simulation of Computer and Telecommunication Systems*, Fort Worth, Texas, October 2002.

[21] Y. Xu, J. Heidemann, and D. Estrin, "Geography-informed energy conservation for ad-hoc routing," *Proc. ACM MobiCom'01*, pp. 70-84, Rome, July 2001.

[22] Y. Yu, D. Estrin, and and R. Govindan, "Geographical and energy aware routing: A recursive data dissemination protocol for wireless sensor networks," *UCLA Computer Science Department Tech. Rep., UCLA-CSD-TR-01-0023*, May 2001.

[23] C. Schurgers and M. B. Srivastava, "Energy efficient routing in wireless sensor networks," *Proc. IEEE MILCOM'01*, 2001.

[24] M. A. Youssef, M. F. Younis, and K. A. Arisha, "A constrained shortest path energy-aware routing algorithm for wireless sensor networks," *Proc. IEEE WCNC'2002*, vol. 2, pp. 794-799, 2002.

[25] F. Ye, A. Chen, S. Lu, and L. Zhang, "A scalable solution to minimum cost forwarding in large sensor networks," *Proc. 10th Intl. Conf. on Comp. Commun. and Networks,* pp. 304-309, 2001.

[26] R. C. Shah and J. M. Rabaey, "Energy aware routing for low energy ad-hoc sensor networks" *Proc. IEEE WCNC'2002*, pp. 350-355, March 2002.

[27] K. Sohrabi, J. Gao, V. Ailawadhi, and G.J. Pottie, "Protocols for self-organization of a wireless sensor network," *IEEE Pers. Commun.,* pp. 16-27, October 2000.

[28] I. Demirkol, C. Ersoy, and F. Alagoz, "MAC protocols for wireless sensor networks: A survey," *IEEE Commun. Mag.,* 2005.

[29] W. Ye, J. Heidemann, D. Estrin, "Medium access control with coordinated adaptive sleeping for wireless sensor networks," *IEEE/ACM Trans. on Networking,* vol. 12, no. 3, 493-506, June 2004.

[30] M. Zorzi, "A new contention-based MAC protocol for geographic forwarding in ad-hoc and sensor networks," *IEEE ICC'04*, vol. 6, pp. 3481-3485, June 2004.

[31] R. Rugin and G. Mazzini, "A simple and efficient MAC-routing integrated algorithm for sensor networks," *IEEE ICC'04*, vol. 6, pp. 3499-3503, June 2004.

[32] S. R. Gandham, M. Dawande, R. Prakash, and S. Venkatesan, "Energy efficient schemes for wireless sensor networks with multiple mobile base stations, *Proc. IEEE GLOBECOM'2003*, pp. 377-381, December 2003.

[33] M. Bhardwaj, T. Garnett, and A. P. Chandrakasan, "Upper bounds on the lifetime of wireless sensor networks," *Proc. IEEE ICC'2001,* 2001.

[34] M. Bhardwaj and A. P. Chandrakasan, "Bounding the lifetime of sensor networks via optimal role assignment," *Proc. IEEE INFOCOM'02*, pp. 1587-1596, 2002.

[35] H. Zhang and J. Hou, "On deriving the upper bound of α-lifetime for large sensor networks," *Proc. ACM MobiHoc'2004*, May 2004.

[36] D. M. Blough and P. Santi, "Investigating upper bounds on network lifetime extension in cell-based energy conservation techniques in stationary ad-hoc networks," *Proc. MobiCom'2002*, September 2002.

[37] V. Rai and R. N. Mahapatra, "Lifetime modeling of a sensor network," *Proc. Design, Automation, and Test in Europe Conf. and Exhibition (DATE'05)*, 2005.

[38] S. Arnon, "Deriving an upper bound on the average operation time of a wireless sensor network," *IEEE Commun. Letters*, vol. 9, no. 2, pp. 154-156, February 2005.

[39] M. Grossglauser and D. N. C. Tse, "Mobility increases the capacity of ad-hoc wireless networks," *IEEE/ACM Trans. on Networking*, vol. 10, no. 4, pp. 477-486, August 2002.

[40] R. Shah, S. Roy, S. Jain, and W. Brunette, "Data mules: Modeling a three-tier architecture for sparse sensor networks," *Proc. IEEE Workshop on Sensor Network Protocols and Applications*, 2003.

[41] W. Zhao and M. H. Ammar, "Message ferrying: Proactive routing in highly partitioned wireless ad-hoc networks," *Proc. IEEE Workshop on Future Trends of Distributed Computing Systems*, 2003.

[42] W. Zhao, M. Ammar, and E. Zegura, "A message ferrying approach for data delivery in sparse mobile ad-hoc networks," *Proc. MobiHoc'04*, pp. 187-198, Japan, May 2004.

[43] A. A. Somasundara, A. Ramamoorthy, and M. B. Srivastava, "Mobile element scheduling for efficient data collection in wireless sensor networks with dynamic deadlines," *Proc. IEEE Intl. Real-Time Systems Symposium*, 2004.

[44] Z. M. Wang, S. Basagni, E. Melachrinoudis, and C. Petrioli, "Exploiting sink mobility for maximizing sensor networks lifetime," *Proc. of 38th Hawaii Intl. Conf. on System Sciences*, 2005.

[45] J. Luo and J.-P. Hubaux, "Joint mobility and routing for lifetime elongation in wireless sensor networks," *Proc. IEEE INFOCOM'05*, 2005.

[46] A. P. Azad and A. Chockalingam, "Mobile base stations placement and energy aware routing in wireless sensor networks," accepted in *IEEE WCNC'2006*, Las Vegas, April 2006.

[47] A. P. Azad and A. Chockalingam, "Energy efficient mobile base stations placement algorithms in wireless sensor networks," *Proc NCC'2006*, pp. 368-372, IIT, New Delhi, January 2006.

[48] A. P. Azad and A. Chockalingam, "Upper bounds on the lifetime and optimal locations of multiple base stations in wireless sensor networks," *being submitted to IEEE GLOBECOM'2006*, San Francisco, 2006.

[49] J. G. Proakis, *Digital Communications,* McGraw-Hill, 1995.

[50] M. K Simon and M.-S. Alouini, *Digital Communications Over Fading Channels: A Unified Approach to Performance Analysis,* Wiley Series, July 2000.

[51] W. C. Jakes, Jr., *Microwave Mobile Communications,* New York: John-Wiley & Sons, 1974.

[52] S. M. Alamouti, "A simple transmit diversity technique for wireless communications," *IEEE Jl. Sel. Areas in Commun.,* vol. 16, no. 8, pp. 1451–1458, October 1998.

[53] V. Tarokh, N. Seshadri, and A. R. Calderbank, "Space-time codes for high data rate wireless communications: Performance criterion and code construction," *IEEE Trans. Inform. Theory*, vol. 44, no. 2, pp. 744-765, March 1998.

[54] A. Sendonaris and E. Erkip, "User cooperation diversity Part I: System Aspects," *IEEE Trans. Commun.,* vol. 51, no. 11, pp., November 2003.

[55] A. Sendonaris and E. Erkip, "User cooperation diversity Part II: Implementation aspects and performance analysis," *IEEE Trans. Commun.,* vol. 51, no. 11, pp. 1939-1948, November 2003.

[56] J. N. Laneman, D. N. C Tse, and G. W. Wornell, "Cooperative diversity in wireless networks: Efficient protocols and outage behavior," *IEEE Trans. Inform. Theory*, 2004.

[57] N. Shastry and R. S. Adve, "A theoretical analysis of cooperative diversity in wireless sensor networks," *Proc. IEEE GLOBECOM'2005*, 2005.

[58] D. B. Shmoys, "Cut problems and their application to divide-and-conquer," *Approximation Algorithms for NP-hard Problems, PWS Publishing Company*, Boston, pp. 192-235, 1997.

[59] G. Even, J. Naor, S. Rao, and B. Schieber, "Fast approximate graph partitioning algorithms," *Proc. Ann. ACM-SIAM Symp. on Discrete Algorithms,* ACM-SIAM, pages 639-648, 1997.

[60] G. L. Nemhauser and L. A. Wolsey, *Integer Programming and Combinatorial Optimization*, Wiley, 1988.

[61] J. Agre and L. Clare, "An integrated architecture for cooperative sensing networks, *Computer*, 33(5), pp. 106-108, 2000.

[62] J. Chlebikova, "Approximability of the maximally balanced connected partition problem in graphs," *Inform. Process. Lett.,* no. 60, pp. 225-230, 1996.

[63] A. Ribeiro, X. Cai, and G. B Giannakis, "Symbol error probabilities for general cooperative links," *IEEE Trans. Wireless Commun.,* May 2005.

[64] R. Annavajjala, P. C. Cosman, and L. B. Milstein, "On the performance of optimum noncoherent amplify-and-forward reception for cooperative diversity," *IEEE MILCOM'2004.*

[65] P. Herhold, E. Zimmermann, and G. Fetweiss, "Cooperative multihop transmission in wireless networks," *Computer Networks,* no. 49, pp. 299-324, 2005.

[66] A. Chandrakasan et al., "Design considerations for distributed microsensor systems," *in Custom Integrated Circuits Conference (CICC),* pp. 279 286, May 1999.

[67] G. L. Stuber, *Principles of Mobile Communication*, Kluwer Academic Publishers, Boston, 1997.

[68] W. Heinzelman, *Application-Specific Protocol Architectures for Wireless Networks*, Ph.D. thesis, MIT, 2000.

Publications from this Thesis

1. A. P. Azad and A. Chockalingam, "Mobile base stations placement and energy aware routing in wireless sensor networks," accepted in *IEEE WCNC'2006*, Las Vegas, April 2006.

2. A. P. Azad and A. Chockalingam, "Energy efficient mobile base stations placement algorithms in wireless sensor networks," *Proc. NCC'2006*, pp. 368-372, IIT, New Delhi, January 2006.

3. A. P. Azad and A. Chockalingam, "Upper bounds on the lifetime and optimal locations of multiple base stations in wireless sensor networks," *being submitted to IEEE GLOBECOM'2006*, San Francisco, 2006.